OXFORD

SOT | Society of Toxicology
www.toxsci.oxfordjournals.org

TOXICOLOGICAL SCIENCES, 167(1), 2019, 211–226

doi: 10.1093/toxsci/kfy230
Advance Access Publication Date: September 9, 2018
Research Article

Genomic Profiling of BDE-47 Effects on Human Placental Cytotrophoblasts

Joshua F. Robinson,[*,†,1] Mirhan Kapidzic,[*,†] Emily G. Hamilton,[*,†] Hao Chen,[*,†] Kenisha W. Puckett,[*,†] Yan Zhou,[*,†] Katherine Ona,[*,†] Emily Parry,[‡] Yunzhu Wang,[‡] June-Soo Park,[‡] Joseph F. Costello,[§] and Susan J. Fisher,[*,†]

[*]Department of Obstetrics, Gynecology, and Reproductive Sciences, Center for Reproductive Sciences, University of California, San Francisco (UCSF), San Francisco, California 94143; and [†]Department of Obstetrics, Gynecology, and Reproductive Sciences, University of California, San Francisco (UCSF), San Francisco, California 94143; [‡]Environmental Chemistry Laboratory, Department of Toxic Substances Control, California Environmental Protection Agency, Berkeley, California 94710; and [§]Department of Neurological Surgery, University of California, San Francisco (UCSF), San Francisco, California 94158

[*]To whom correspondence should be addressed at Department of Obstetrics, Gynecology, and Reproductive Sciences, Center for Reproductive Sciences, University of California, San Francisco (UCSF), Box: 0665, Bldg: 513 Parnassus Ave, San Francisco, CA 94143-0665. Fax: (415) 476-1635. E-mail: joshua.robinson@ucsf.edu.

ABSTRACT

Despite gradual legislative efforts to phase out flame retardants (FRs) from the marketplace, polybrominated diphenyl ethers (PBDEs) are still widely detected in human maternal and fetal tissues, eg, placenta, due to their continued global application in consumer goods and inherent biological persistence. Recent studies in rodents and human placental cell lines suggest that PBDEs directly cause placental toxicity. During pregnancy, trophoblasts play key roles in uterine invasion, vascular remodeling, and anchoring of the placenta-fetal unit to the mother. Thus, to study the potential consequences of PBDE exposures on human placental development, we used an *in vitro* model: primary villous cytotrophoblasts (CTBs). Following exposures, the endpoints that were evaluated included cytotoxicity, function (migration, invasion), the transcriptome, and the methylome. In a concentration-dependent manner, common PBDE congeners, BDE-47 and -99, significantly reduced cell viability and increased death. Upon exposures to sub-cytotoxic concentrations ($\leq 5\,\mu M$), we observed BDE-47 accumulation in CTBs with limited evidence of metabolism. At a functional level, BDE-47 hindered the ability of CTBs to migrate and invade. Transcriptomic analyses of BDE-47 effects suggested concentration-dependent changes in gene expression, involving stress pathways, eg, inflammation and lipid/cholesterol metabolism as well as processes underlying trophoblast fate, eg, differentiation, migration, and vascular morphogenesis. In parallel assessments, BDE-47 induced low-level global increases in methylation of CpG islands, including a subset that were proximal to genes with roles in cell adhesion/migration. Thus, using a primary human CTB model, we showed that PBDEs induced alterations at cellular and molecular levels, which could adversely impact placental development.

Key words: placenta; cytotrophoblast; transcriptomics; polybrominated diphenyl ether; BDE-47; human; invasion; migration; *in vitro*; methylation.

Despite efforts to the contrary, the continued use of polybrominated diphenyl ethers (PBDEs) as flame retardants (FRs) in consumer goods warrants great concern (Jinhui *et al.*, 2015). Due to their bio-persistence these compounds continue to be identified in human maternal and fetal tissues (Zota *et al.*, 2013). In particular, of the 209 unique PBDE congeners, BDE-47 is found at the highest levels in the majority of US mothers and/or their offspring (Frederiksen *et al.*, 2009; Woodruff *et al.*, 2011; Zota *et al.*, 2018).

Numerous toxicological (Dingemans *et al.*, 2011) and epidemiological (Cowell *et al.*, 2015; Herbstman and Mall 2014) studies indicate that exposures to PBDEs *in utero* may be harmful to the developing human fetus. The ramifications of their bioaccumulation remain largely unknown. In human cell lines and/or animal models, common PBDEs congeners elicit developmental toxicity through several mechanisms, eg, alterations in thyroid hormone (TH) signaling, inflammation, oxidative stress, and epigenetic modifications (Costa *et al.*, 2014). Further investigations are needed to clarify targeted tissues/cell populations and windows of sensitivity during human pregnancy.

The placenta is essential for normal fetal development, and pregnancy complications linked with abnormal placentation are negatively associated with neonatal, child, and adult health (Vinnars *et al.*, 2014). Data generated in rodent models and human cell lines (Kalkunte *et al.*, 2017; Rajakumar *et al.*, 2015; Yang *et al.*, 2006) suggest that environmental compounds are toxic to the placenta. In humans, the placenta is in direct contact with maternal blood in which these chemicals are routinely detected. Thus, it is not surprising that PBDEs are regularly identified in human placentas (Leonetti *et al.*, 2016). While the consequences associated with exposures *in utero* are unknown, recent studies in mammalian models suggest that BDE-47 may alter placental development, causing oxidative stress and inflammation (Park *et al.*, 2014; park and Loch-Caruso, 2014) as well as perturbing hormone signaling (park and Loch-Caruso, 2015).

During pregnancy, the placenta undergoes numerous morphological and molecular transformations to support the growing demands of the developing fetus. Specialized placental cells known as cytotrophoblasts (CTBs) are critical for: (1) initiating and maintaining the physical anchor between the fetal and maternal units; (2) penetration and invasion into the uterine wall; and (3) remodeling of the uterine vascular architecture to reroute maternal blood flow to the placenta (Red-Horse *et al.*, 2004, 2005). Perturbations in CTB development may underlie several pregnancy complications, including: preeclampsia (PE; Fisher, 2015), intrauterine growth restriction (IUGR), preterm birth (Romero *et al.*, 2014) and over aggressive CTB invasion (Jauniaux and Jurkovic, 2012). *In vitro*, isolated cultured primary human villous CTBs (Fisher *et al.*, 1989; Hunkapiller and Fisher, 2008; Kliman *et al.*, 1986) have been proposed as a model of placentation.

CTB invasion is a complicated process with many components, some of which are unique. The cells must exit the placenta, crossing over to the uterus, where they attach to its surface before they deeply invade the parenchyma. This process is accompanied by a series of molecular transformations, involving relevant pathways, including cell-cell adhesion, migration/invasion, and vascular remodeling (Maltepe and Fisher, 2015). Upon isolation and culture, villous CTBs differentiate along the invasive pathway, modulating the same sets of molecules that mediate this process *in vivo* (Robinson *et al.*, 2017).

Genomic profiling of isolated CTBs revealed dramatic shifts at transcriptomic and epigenomic levels across gestation including many key molecules with known functional roles in placental development and disease (Roadmap Epigenomics *et al.*, 2015). In assessing environmental chemical impacts during development, the incorporation of genomic-based approaches in toxicological studies, ie, toxicogenomics, provides a global analysis of molecular response to environmental exposures (Robinson and Piersma, 2013). Given the unusual dynamics of the CTB genome, the potential for environmental chemicals to influence chromatin architecture/gene expression, and the links between placental health and successful birth outcomes (Burton *et al.*, 2016; Kovo *et al.*, 2012), investigations are needed to address potential interactions between these important variables.

Here, we used a cell culture model to study the effects of PBDEs on CTB differentiation and invasion. Acute exposures resulted in accumulation of the parent compound and minimal metabolism. Subcytotoxic concentrations of BDE-47 impaired the ability of CTBs to migrate and invade. These functional alterations were accompanied by alterations at transcriptomic and epigenomic levels. Together these data suggest that PBDE exposures could impact process and pathways that are integral to the placenta's role in governing pregnancy outcome.

MATERIALS AND METHODS

Tissue collection. All methods were initially approved by the UCSF Institutional Review Board. Informed consent was obtained from all donors. Second trimester placentas intended for cell isolations were collected immediately following elective terminations and placed in cytowash medium, consisting of DME/H-21 (Gibco), 12.5% fetal bovine serum (Hyclone), 1% glutamine plus (Atlanta Biologicals), 1% penicillin/streptomycin (Invitrogen), and 0.1% gentamicin (Gibco). Tissue samples were placed on ice prior to dissection.

Human primary villous cytotrophoblast isolation. CTBs were isolated from second trimester human placentas as described previously (Robinson *et al.*, 2017). Single cells were counted using a hemacytometer and immediately transferred to a Matrigel (BD biosciences)-coated 12-well plate. CTBs were cultured at a density of 500 000 CTBs/well in 1.5 ml medium containing DME/H-21, 2% Nutridoma (Roche), 1% sodium pyruvate (Sigma), 1% Hepes buffer (Invitrogen), 1% glutamate plus (Atlanta Biologicals), and 1% penicillin/streptomycin (Invitrogen). Cells were incubated at 37°C in 5% CO_2/95% air. We immunostained with anti-cytokeratin (CK; anti-CK rat polyclonal; 1:100, Damsky *et al.*, 1992), a marker regularly used to detect for relative trophoblast purity (~ 80–90% CTBs) in our cultures across experiments. Cell preparations not meeting this criteria were not used for downstream analyses.

Chemicals. PBDE congeners, BDE-47 (2,2′4,4′-tetrabromodiphenyl ether, >99%, CAS #5436-43-1, AccuStandard) and BDE-99 (2,2′4,4′,5-pentabromodiphenyl ether, >99%, CAS #60348-60-9, AccuStandard), bisphenol A (BPA; >99%, #80-05-7, Sigma), and perfluorooctanoic acid (PFOA, >96%; #335-67-1, Sigma) were dissolved in dimethyl sulfoxide (DMSO, Sigma-Aldrich) to make stock solutions and serial dilutions for all experimental studies. Chemical exposures were introduced at a 1:1000 (vol/vol) media dilution for all assessments.

Cytotoxicity assessments. Freshly isolated CTBs were cultured for 15 h ($t_{15\ h}$) and supplied with new media containing: media only (control), DMSO (vehicle control; 0.1%), BDE-47 (0.1, 1.0, 10, 25 μM), BDE-99 (0.1, 1.0, 10, 25 μM), BPA (0.1, 1.0, 10, 100 μM), or PFOA (1, 10, 25, 100, 250, 1000 μM). At $t_{15\ h}$, cultured CTBs are actively aggregating, one of the initial steps in differentiation/invasion. We evaluated cytotoxicity after a 24-h exposure due to previous studies suggesting that this time point was optimal to detect significant changes, at cellular and molecular levels, in developing *in vitro* systems (Costa *et al.*, 2015; park and Loch-Caruso, 2014). We measured cell viability using the neutral red (NR; 40 ng/ml, VWR) lysosomal uptake assay (Borenfreund and Puerner, 1985). Briefly, after 24 h, the media was removed and wells were gently washed with PBS to eliminate residual compound. New media containing NR was added to each plate and

incubated for 2 h at 37°C. Cells were washed with PBS and a 50% ethanol/1% acetic acid solution was added to release the NR dye, which was measured at an absorbance of 540 nM via a spectrophotometer (Biotek Epoch). In parallel, in exposed and control CTB cultures, we evaluated lactate dehydrogenase (LDH) activity—a marker of cell death—within the supernatant using the Cytotoxicity Detection Kit (Roche) following the recommended manufacturer protocol. Absorbance readings for LDH were acquired at 490 nM. For both cytotoxicity endpoints, within each experiment, background absorbance readings were subtracted from mean absorbance values. Adjusted values were normalized as compared with the control (= 100%). Average relative percentages and corresponding standard error (SEM) were computed across the independent experiments ($n \geq 3$). Additional pilot investigations were completed where the initial exposure occurred after 3 h ($t_{3\ h}$) post-plating, before CTB aggregation occurs. No differences in CTB sensitivity to PBDE-induced cytotoxicity were apparent in regards to when the exposure was initiated ($t_{3\ h}$ vs $t_{15\ h}$). We calculated benchmark concentrations (BMCs) for 50% cell viability or 200% LDH activity via asymmetrical dose-response modeling (Graphad Prism 7.0; Giraldo *et al.*, 2002).

PBDE accumulation and metabolism in CTBs. We tested for PBDE concentrations in cell and media fractions of CTB cultures exposed to 0.1% DMSO, BDE-47 1 or 5 μM after 24 h. We evaluated samples for BDE-47, related metabolites, ie, 5-OH-BDE-47 and 6-OH-BDE-47, as well as major PBDE congeners, eg, BDE-17, -28, -66, -85, -99, -100, -153, -154, -183, -196, -197, -201, -203, -206, -207, -209. PBDE concentrations were measured using gas chromatography/high resolution double-focusing sector mass spectrometry (GC-HRMS, DFS, Thermo Fisher, Bremen, Germany) at the Department of Toxic Substances Control (DTSC; Berkeley, California) as described previously (Zota *et al.*, 2013). Average concentrations in cell and media fractions were determined across three independent experiments ($n = 3$). Mass estimates of BDE-47 in cell/media fractions were calculated using chemical concentrations (μg/μl) and the molecular weight (489.79 g/mol) of BDE-47. Percent recovery was estimated to be within ~10% of the expected total amount (media + cell fraction).

Migration of PBDE-exposed CTBs. We evaluated the effect(s) of BDE-47 exposures on CTB migration/aggregation as described previously (Robinson *et al.*, 2017). In brief, we exposed cells with 1% DMSO, 1 or 5 μM of BDE-47 after early attachment ($t_{1\ h}$). Controls containing media only were also ran in parallel. At 5 or 15 h post-exposure, the culture media was removed and CTBs were washed once with PBS to remove residual chemical. Next, CTBs were fixed with 4% paraformaldehyde (PFA, 20 min). Cultures were washed again with PBS (2×) and stored (in PBS) at 4°C until further processing. Cold methanol was added to permeabilize the CTBs. Cultures were washed with PBS (3×) and a PBS-Hoechst 33342 (Life Technologies, 1:2500) solution was added. After 10 min, the liquid was removed and cultures were placed in PBS. For each well, 42 tethered fluorescent images consisting of a 5 mm^2 area were captured using a Leica inverted microscope with a 10× objective and the tiles can function (Leica Application Suite Advanced Fluorescence). Within each image, we identified all cells or "objects" via detection of Hoescht (nuclear-binding dye) using Volocity software (PerkinElmer; version 6.3). We applied automated erosion and division operational functions to enable improved measurements of aggregated cell populations. Objects that intersected with the border of the image or that were initially <20 μm^2 were eliminated from the analysis to limit potential artifacts. Images containing irregularities, eg, cell debris, high background, blurry features, were also removed (<5% of images). We evaluated ~20 000 cells per well. The minimum distance between nuclei (centroid to centroid) was evaluated using an automated process which measured all possible distances between objects within each image. We identified the average cell number per image in each independent experiment and removed images outside the normal range (mean ±1.5 SD; ~5% of images) to minimize the influence of density as a factor of cell-cell proximity. Within each experiment, we calculated the difference in the average minimum distance among cells exposed to DMSO or BDE-47 versus the media only control. The standard error (SE) to the mean was computed across the average of the six independent experiments. We applied ANOVA and pairwise Student paired *t*-tests to determine significant differences in migration between controls and BDE-47 exposed CTBs ($p < .05$; JMP 13.0).

Invasion of PBDE-exposed CTBs. As described previously (Hromatka *et al.*, 2013), we evaluated the influence of PBDE exposures on the ability of CTBs to invade. We used transwell inserts (8 μm pore size, 24-well plate, Corning Costar) pre-coated with 8 μl of diluted Matrigel™ (3:1 v/v in serum-free medium BD Biosciences) for 20 min at 37°C. CTBs at a density of 250 000 cells in 250 μl media were added into the upper compartment of inserts and placed in 24-well plates containing 800 μl of media per well. After attachment (~$t_{1\ h}$), CTBs were exposed to media only (control), 0.1% DMSO, or BDE-47 (1, 5 μM). After an additional 40 h at 37°C, cells were fixed with 3% PFA (30 min), washed in PBS (2×), and stored in PBS at 4°C until further processing. We quantified CTB projections using immunofluorescence, microscopy, and high-content analysis (Volocity). After PBS removal, cold methanol was added to permeabilize the CTBs (5 min). Cells were washed with PBS (3×) and 5% bovine serum albumin (BSA) (Hyclone)/PBS was added to block nonspecific reactivity. After 1 h, the solution was removed and the primary antibody, anti-CK (Fisher_001-clone7D3, RRID: AB_2631235, rat monoclonal; 1:100 [Damsky *et al.*, 1992]) in 5% BSA was added and incubated overnight at 4°C. The next day, cultures were washed with PBS (3×), inserts were cut using a razor blade, probed with Vectashield containing Dapi (Vector Bio-Labs), and cover slipped. Images were acquired using a Leica inverted microscope (20×) per slide. Invading CTBs and/or significant cell protrusions that reached the underside of the filter were counted using Volocity software (PerkinElmer; version 6.3) and preset optimized criteria (area > 4000 μm^2; max pixel intensity > 75; shape factor > 0.75). All images and generated counts were double checked manually to assure proper identification. Within each independent experiment ($n = 3$), we determined the total CTB protrusions per condition across three technical replicates (5 images per slide). Invasion was expressed as a ratio in CTB protrusions per image between each exposure group and the media only control (= 100%) per experiment. The standard error (SE) to the mean was computed across the average of the experiments. Significant effects were determined via ANOVA and Student *t*-tests between PBDE exposure groups and the vehicle control ($p < .05$; JMP 13.0).

RNA isolation from CTBs. We isolated RNA from CTBs exposed to BDE-47 and controls for downstream microarray or qRTPCR gene expression assessments. CTBs were cultured for 3 h ($t_{3\ h}$) or 15 h ($t_{15\ h}$) and supplied with new media containing: media only (control), DMSO (vehicle control), and/or BDE-47 (0.1–10 μM). Initiated exposure times in culture were selected due to our previous analyses (Robinson *et al.*, 2017), indicating that in unexposed cultures, single CTBs attach and begin to migrate at

~3 h in culture, and at ~15 h, aggregation and cell remodeling actively occur. We isolated RNA from CTBs for transcriptomic and qRT-PCR investigations. Samples used for transcriptomic studies consisted of cells (1) exposed to either DMSO or BDE-47 (1 μM); (2) from an independent placenta ($n = 3$); and (3) varied in age during the second trimester (gestational week [GW] 16.6, 19.3, or 21.6). In total, 12 samples were used for microarray analyses (Supplementary Table 1). Additional samples for qRT-PCR validation were also generated from individual placentas and ranged from GW 14–22. To isolate RNA, in brief, immediately following a 24 h exposure duration, the media was removed and RLT Lysis Buffer (Qiagen) was directly added to the culture dish. The lysate was collected and stored at −80°C. RNA was purified using the RNeasy Micro Kit (Qiagen). The RNA concentration and quality were estimated (absorbance 260 nm/280 nm = 1.9–2.1) by using a Nanodrop spectrometer (Thermo Scientific). Samples destined for microarray analyses were assessed for quality (RIN > 9) using the Agilent RNA 6000 Nano LabChip Kit and Bioanalyzer 2100 system.

Gene expression profiling of BDE-47-exposed CTBs. We evaluated the effects of BDE-47 exposure on the global transcriptome in CTBs using the Affymetrix Human Gene 2.0 ST array platform. Sample processing and hybridization was performed by the UCSF Gladstone Institute as described previously (Winn *et al.*, 2007). Affymetrix CEL files were processed using the Affymetrix Expression Console and Transcriptome Analysis Console (TAC) software packages. Raw values were normalized via the robust multi-array average (RMA) algorithm. Raw and normalized data were deposited in the Gene Expression Omnibus (GEO; GSE104896). We analyzed probes with median intensities >20% of the total distribution and discarded duplicates probes representing the same transcript by using the most variable probe within the full sample set. In total, we examined 27 729 unique genes using this approach. A multivariate ANOVA model was applied [y(expression) = B_1x(exposure) + B_2x(time) + B_3x(placenta)] to identify differentially expressed (DE) genes due to BDE-47 or time, while adjusting for differences across genetically unique placental cell preparations, ie, batch effects. Average fold change (FC) values were determined by calculating the average ratio of the difference of log 2 intensities between BDE-47 (1 μM) and the respective vehicle control within each experiment. We defined DE genes due to BDE-47 exposure (BDE-47 DE Genes) by applying a cutoff of $p \leq .025$ (unadjusted) and an absolute average FC ≥ 1.25 between BDE-47 and DMSO for both of the two exposure scenarios, ie, initiated either at $t_{3\ h}$ or $t_{15\ h}$. Approaches used to control for false positives (eg, Bonferonni) were not applied because a limited number of genes passed standard criteria thresholds (FDR < 5%), a common observation in toxicological studies using primary human *in vitro* systems. Thus, downstream analyses focused on validated targets and changes in related enriched functional pathways. Hierarchical clustering of FC values was completed by using average linkage and Euclidean distance (TIGR MEV; Saeed *et al.*, 2006). We conducted functional enrichment of Gene Ontology (GO) Biological Processes (Level 4) of BDE-47 DE Genes defined using the Official Gene Symbol (OGS) using DAVID (Huang *et al.*, 2007). GO terms containing ≥ 7 DE Genes and an enrichment significance of $p \leq .01$, were selected as significantly overrepresented. Corresponding enrichment scores, ie, p-values, were also determined for up- and downregulated gene clusters. We grouped terms based on GO classification (Gene Ontology Consortium, 2015) and identified parent GO terms to define themes.

Transcription factor binding site enrichment analysis of BDE-47 DE genes. We identified potential upstream regulators, ie, TFs, of genes found to be DE due to BDE-47 exposure in our transcriptomic analyses using OPOSSUM. Enriched TFBS motifs were defined as (1) -2000 bases upstream of the transcription start site (TSS); (2) an identification score of ≥ 0.4; and (3) an enrichment score of Z ≥ 7, which indicates the over-occurrence of the TFBS in BDE-47 genes/sequences as compared with the background total genome. Within this subset of related TFs, we explored transcript abundance in CTBs isolated from second trimester versus term human placentas using an RNA-seq dataset previously generated in our laboratory (Roadmap Epigenomics *et al.*, 2015). Expression data was processed as described previously (Robinson *et al.*, 2016). Abundance and significance of differential expression between second trimester versus term was determined using DESeq2 and Wald's test (Chen *et al.*, 2011).

Targeted validation of BDE-47 DE genes in CTBs. Using CTBs from independent placentas ($n \geq 3$) in addition to samples employed in the microarray analyses, we investigated expression levels of target genes in control and BDE-47 (1 μM, initiated at $t_{3\ h}$; 0.01–10 μM, initiated at $t_{15\ h}$) exposed-samples at 24 h to validate microarray analyses and further interrogate the concentration-response of CTBs to BDE-47, including at more physiologically relevant levels. Using purified samples, we converted RNA to cDNA using ISCRIPT Universal TaqMan (Bio-Rad), and performed qRT-PCR via TaqMan primers for FABP4, FABP7, GPR34, GREM1, HMGCS1, IL6, MMP1, NEUROD2, PLAC4, and SCD (Supplementary Table 2) mixed with TaqMan Universal Master Mix II, no UNG (Life Technologies). Reactions were carried out for 40 cycles. A minimum of 3 technical replicates were analyzed for all comparisons. Differential expression between PBDE-exposed and controls was calculated via the ΔΔCT method: (1) normalized to geometric mean of housekeeping genes, GAPDH and ACTB; and (2) adjusted to the vehicle control (DMSO) for each experiment. Housekeeping genes were selected due to their common application in experiments employing reproductive tissues/cells (Arenas-Hernandez and Vega-Sanchez 2013) and the fact that our microarray data showed that their expression was not significantly altered by BDE-47 exposures (not shown). To determine significant changes across concentrations BDE-47, we employed ANOVA (JMP). FC values were expressed as average log 2 ratios between each exposure group and the vehicle control.

DNA isolation of BDE-47-exposed CTBs. Following exposure to BDE-47 (1 μM) or vehicle for 24 h (initiated at $t_{3\ h}$ or $t_{15\ h}$), CTBs ($n = 3$ independent experiments) were washed with PBS and collected using a cell scraper. Cells (~1 million per sample) were suspended in 10 ml of PBS, pelleted (800 rpm, 5 min), washed 2× with PBS and stored at −80 C. To extract genomic DNA, CTBs were digested with 1 mg/ml proteinase K in lysis buffer (50 mM Tris, pH 8.0, 1 mM EDTA pH 8.0, 0.5% SDS) overnight at 55°C. Following RNase treatment, DNA was isolated using the Phenol-Chloroform Isoamyl Alcohol (PCI) method, followed by precipitation with ethanol, and resuspended in TE. DNA quality was evaluated via Nanodrop and the Agilent RNA 6000 Nano LabChip Kit and Bioanalyzer 2100 system.

Methylation profiling of BDE-47-exposed CTBs. Downstream processing of genomic DNA bisulfite conversion was performed using the EZ DNA Methylation Kit (ZymoResearch) and Infinium HumanMethylation450 bead arrays (Illumina) following the manufacturer's protocols. Methylation data was processed via

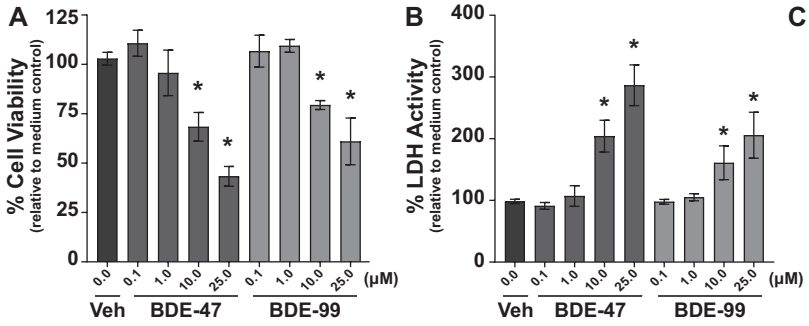

	BMC_{50} Viability	BMC_{200} LDH
BDE-47	18.1μM	12.5μM
BDE-99	33.5μM	24.6μM
BPA	116.5μM	96.6μM
PFOA	363.8μM	432.9μM

Figure 1. Concentration-dependent CTB cytotoxicity induced by PBDEs. (A) CTB viability or (B) LDH activity at 24 h in cultures that contained PBDEs or 0.1% DMSO (vehicle control, VEH) relative to medium with no additives. The standard error (SE; black bars) of the mean was computed across experiments ($n \geq 4$). Asterisks (*) indicate significant differences between tested concentrations of PBDEs and vehicle control ($p \leq .05$). (C) Benchmark chemical concentrations (BMCs) corresponding to a 50% loss of viability or a 200% increase in LDH activity.

Illumina standard background subtraction and control probe normalization, and converted to M values, using the minfi package and BRB Array Tools (Simon *et al.*, 2007). Probes that mapped to regions of sex chromosomes were eliminated from the analysis. Similar to the model used for transcriptomic analyses, we utilized a fixed effect multivariate model (using M-value = ratio of methylated probe vs unmethylated probe intensities) to identify differentially methylated (DM) CpGs due to exposure or time, while controlling for baseline differences across CTBs from genetically unique placentas. Beta values, which reflect the proportion of methlyated probes (ranging from 0 to 1) were determined via logit transformation ($\log_2(M/(M+1))$ of M-values (Du *et al.*, 2010). The change in methylation was determined by subtracting β values between BDE-47 (1 μM) and the respective vehicle control within each experiment. Significant DM CpGs were identified using a $p \leq .005$ (unadjusted) and average absolute $\beta \geq 0.025$ between BDE-47 and DMSO for both exposure windows, ie, initiated either at $t_{3\ h}$ or $t_{15\ h}$. We evaluated enrichment of DM CpGs by chromosome location (Fisher's exact test). We interrogated genes in proximity to DM CpGs for functional relevance using DAVID (Biological Level 4). These analyses were also conducted for the subset of DM CpGs located proximal to promoter regions of genes, defined to be located <1500 b upstream of the TSS, 5′ untranslated region (UTR), or first Exon. Raw and normalized data were deposited in the NCBI GEO repository GSE115399.

We examined correlations between mRNA expression and DM CpGs by aligning the datasets based on associated OGS annotation. For the subset of DM CpGs in proximity of promoter regions, we assessed the influence of BDE-47 exposures on expression in comparison with the change in methylation at each independent CpG island.

RESULTS

Concentration-Dependent PBDE-Induced Cytotoxicity in CTBs

After 24 h, we evaluated the effects of BDE-47 or -99 (0.1–25 μM) exposures on CTB viability and death using the neutral red and LDH activity assays, respectively. In a concentration-dependent manner, both PBDE congeners significantly reduced cell viability (ANOVA, $p < .05$; Figure 1A) and increased LDH activity (Figure 1B). In general, the two congeners displayed similar potencies ($p \geq .05$). *Post-hoc* analyses (*t*-test) comparing cultures exposed to PBDE versus vehicle control (1% DMSO) revealed concentrations ≥ 10 μM of BDE-47 or -99 to be significantly cytotoxic. In pilot investigations, sensitivity was not dependent on exposure window (initiated at $t_{3\ h}$ vs $t_{15\ h}$; not shown). Comparisons of BMCs associated with a 50% loss in cell viability or 200% increase in LDH activity, suggested that CTBs were more sensitive to PBDEs versus other common endocrine disruptors (BPA or PFOA) *in vitro* (Figure 1C). Overall, our analyses indicated that PBDEs were relatively potent EDCs that induce concentration-dependent cytotoxicity in CTBs. Due to similarities in cytotoxic profiles between BDE-47 and -99 and previous studies indicating BDE-47 to be the highest detected congener in human placentas (Zota *et al.*, 2018), we focused our efforts on BDE-47 effects, at functional and molecular levels, in CTBs.

Partitioning of BDE-47 in Isolated CTBs and Their Culture Medium

Using gas chromatography-mass spectrometry, we evaluated: (1) BDE-47; (2) hydroxylated metabolites of the parent species; and (3) other PBDE co-contaminants, in CTBs and their culture medium, which contained subcytotoxic concentrations of BDE-47 or vehicle (0.1% DMSO). First, we quantified BDE-47 in the medium after 24 h of exposure to 1 or 5 μM of this compound. In both cases, the measured amounts were less than the input: 0.7 ± 0.3 μM or 1.2 ± 0.2 μM, respectively (Figure 2A). Second, we plotted the mass distribution (in μg) of BDE-47 in the medium and cells versus the expected recovery (Figure 2B) also at 24 h. Quantification of BDE-47 in the exposed cultures revealed 0.5 ± 0.2 μg (1 μM) and 0.9 ± 0.1 μg (5 μM) in the medium, and 0.3 ± 0.2 μg (1 μM) and 3.1 ± 0.3 μg (5 μM) in the cells. At the concentrations tested, total recovery (medium + cells) was within 10% of expected estimates (black bars). This suggested an ~10× increase in CTB accumulation of BDE-47 at the 5 μM versus the 1 μM exposure. Overall, our results suggested bioaccumulation of BDE-47 in the cells and that the uptake rate was nonlinear and concentration dependent.

In general, hydroxylated metabolites of BDE-47 (5-OH, 6-OH) were not detected at appreciable levels. The metabolite 6-OH-BDE-47 was identified in one of the three CTB samples that were analyzed, which was 0.0003% of the ∑BDE-47 recovered. In addition to BDE-47, four of the eighteen PBDE congeners evaluated, ie, -17, 28, -85, -99, were detected at low levels in the majority of all samples, which was <0.4% of the ∑PBDEs (Supplementary Table 3). PBDE concentrations were below the minimum detection level (MDL) in all samples exposed to the vehicle control, evidence that congeners other than BDE-47, which were detected in the exposed CTBs, were contaminants of the chemical stock. These results suggested that CTBs had little to no hydroxylated metabolism of the parent compound during 24 h of exposure.

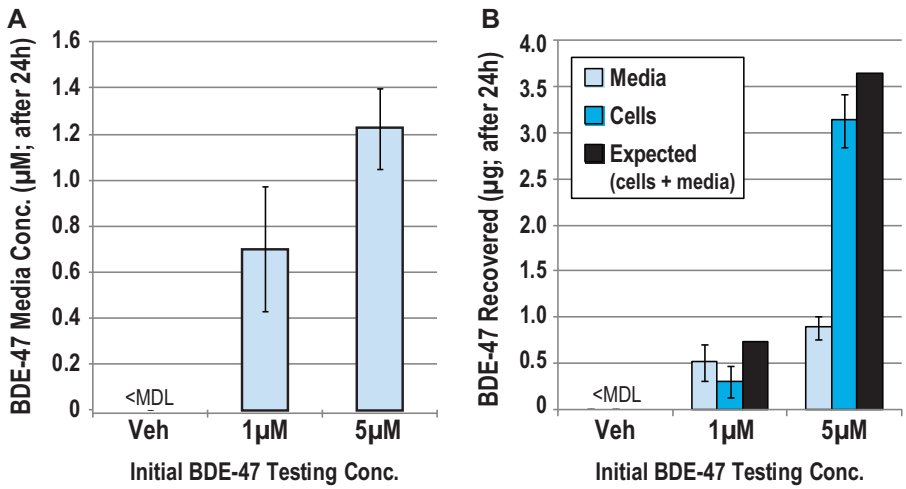

Figure 2. Bioaccumulation of BDE-47 in CTBs. A, CTBs were cultured for 24 h in BDE-47 (1 or 5 µM) or DMSO (0.1%). Gas chromatography-mass spectrometry enabled measurements of the compound amount in each conditioned medium sample. B, Distribution of BDE-47 in the medium (light shading) or cells (dark shading) versus the expected recovery in both compartments (black bars). In general, the hydroxylated metabolites (6-OH-BDE-47 and 5-OH-BDE-47) were not detected. MDL, Minimum level of detection.

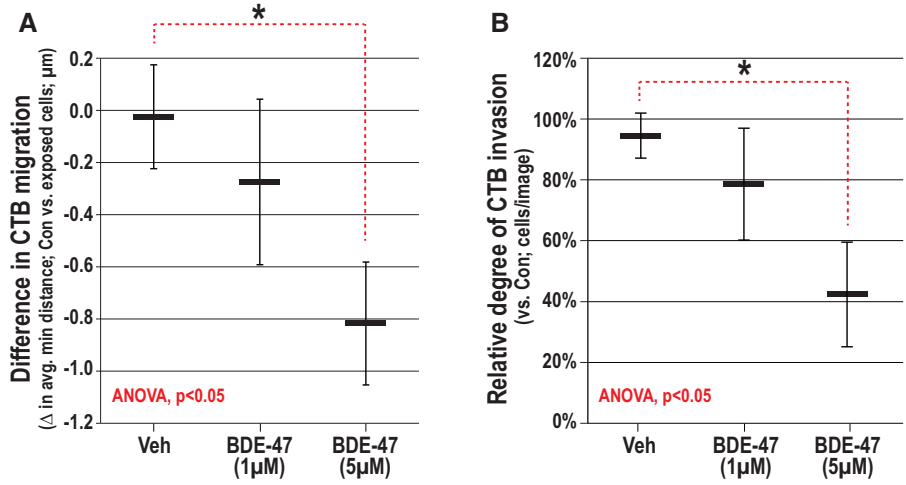

Figure 3. Concentration-dependent effects of BDE-47 on CTB migration and invasion. A, The minimum distance between CTBs exposed to BDE-47 (1 or 5 µM) or vehicle (0.1% DMSO) following 5 h exposure durations. B, The average number of identified projections per image in BDE-47 exposed and control cultures after 40 h. Asterisks signify significant effects between tested concentrations and vehicle control (*t*-test, $p \leq .05$). The standard error (SE) of the mean was computed across independent experiments ($n \geq 4$).

BDE-47 Effects on CTB Migration and Invasion

Under control conditions, CTBs plated on Matrigel™ migrate toward one another at a rate of ~0.3 µm/h, forming multicellular aggregates during the first 15 h of culture. Significant inhibition of migration/aggregation was observed with BDE-47 after 5 h exposure (ANOVA, $p < .05$). Pairwise comparisons between specific concentrations of BDE-47 and vehicle control indicated that 5 µM significantly reduced migration (Δ in average minimum distance = 0.8 µm; $p < .05$), while 1 µM caused only a modest reduction in inhibition (Figure 3A). At 15 h, differences in CTB migration were not observed across groups (not shown), suggesting the ability of CTBs to compensate for the differences that were initially observed. In addition, using a transwell culture system, we assessed BDE-47 effects on the cells' ability to invade. After 40 h exposure, with 1 µM BDE-47, there was no difference between the levels in experimental versus control cultures. In contrast, 5 µM significantly impaired invasion (42% of media only control; $p < .05$, Figure 3B). Our results suggested that BDE-47 perturbs CTB migration and invasion in a concentration-dependent manner.

Global Expression Profiling of BDE-47 in CTBs

CTBs were plated for 3 or 15 h before they were exposed for 24 h to BDE-47 (1 µM) or vehicle (0.1% DMSO) after which global gene expression profiling was performed. We applied a fixed effects linear model (ANOVA) to identify BDE-47 responsive transcripts. In total, the expression of 276 genes was significantly altered ($p \leq .025$, absolute FC $\geq$ 1.25). Hierarchical clustering showed that 159 genes were upregulated and 117 genes were

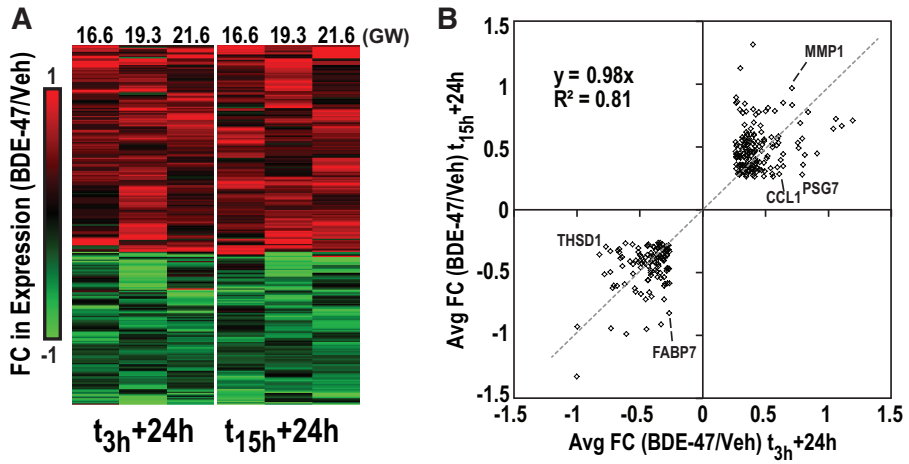

Figure 4. Gene expression profiling of BDE-47-exposed CTBs. A, Cultures were exposed to 1 μM BDE-47 for 24 h starting either 3 or 15 h after they were plated. Global transcriptional profiling showed that 276 genes were DE as compared to CTBs that were cultured in 0.1% DMSO ($p \leq .025$, absolute FC ≥ 1.25). Hierarchical clustering demonstrated similar responses among the CTB cultures and between the two exposure windows. FC ratios are displayed as the log 2 difference between BDE-47 (1 μM) and the vehicle control for each experiment. B, Correlations between the average gene expression FC responses for the different exposure windows. Red (upregulated genes); green (downregulated genes); GW gestational week.

downregulated (Figure 4A). On average, responses to BDE-47 were independent of when exposures were initiated ($y = 0.98x$, $R^2 = 0.81$; Figure 4B). Thus, BDE-47 induced significant transcriptomic alterations in cultured CTBs and these changes occurred irrespective of the exposure window.

GO Analyzes of BDE-47 Responsive Genes

Genes whose expression was modulated by BDE-47 were mapped into GO terms. The majority of enriched biological processes were driven by upregulated transcripts. They included morphogenesis, vasculature development, cell differentiation, cell migration, signal transduction, inflammatory response, protein metabolism, and regulation of biosynthetic process-related terms ($p \leq .01$; # of genes changed within each GO term ≥ 7; Figure 5A). Fewer enriched biological processes were driven by downregulated genes. In general, these GO terms were related to lipid and steroid metabolism.

Next, we clustered genes belonging to GO terms related to important aspects of CTB biology and placental toxicology: morphogenesis, vasculature development, cell migration, inflammatory responses, and cellular lipid metabolic processes (Figure 5B). Forty-one genes were included in this subset. This analysis highlighted BDE-47-induced perturbations in the expression of genes involved in: (1) trophoblast differentiation (eg, MMP1, MMP8, TEK, NODAL, BMP2); (2) inflammatory pathways (eg, CCL13, IL1A, IL6, IL1RN, CCL1); and (3) lipid/steroid metabolism (eg, FABP4, FABP7, FASN, INSIG1, HMGCS1). From this group we selected seven genes (in italics) and an additional two targets (GPR34, PLAC4) to further interrogate the concentration-response relationship of BDE-47 exposures (0.1–10 μM) and mRNA expression. We observed significant effects for the 9 targets, 8 of which had monotonic relationships with BDE-47 exposures (ANOVA, $p \leq .05$). Specifically, IL6, MMP1, GREM1, and PLAC4 were significantly upregulated; GPR34, SCD, HMGCS1, and FABP7 were significantly downregulated (Figure 5C). Minimal changes were observed at concentrations ≤0.1 μM. Trends in response to BDE-47 (1 μM) were similar for the two exposure windows initiated at 3 or 15 h. The qRT-PCR results positively correlated with the microarray data ($R^2 = 0.74$; Supplementary Figure 1). Thus, our findings suggested specific pathways with known roles in trophoblast development and/or PBDE-induced toxicity were significantly altered by exposure to this compound.

Transcription Factor Binding Site (TFBS) Enrichment Analysis of BDE-47 Responsive Genes

Given the important role of transcription factors in regulating gene expression and chemical responses, we analyzed the TFBSs of genes that encoded mRNAs whose abundance changed due to BDE-47 exposure. Ten of these motifs for human TFs were enriched in this gene subset ($Z \geq 7.0$; Table 1). Based on our RNA-seq data for second trimester and term CTBs (GEO accession number), nine were among the most highly expressed transcripts (>33% percentile of RNA counts); four (PBX1, RORA, NFKB, TCFCP2L1) were significantly DE between second trimester and term ($p \leq .05$, highlighted). NFYA (Vaiman *et al.*, 2013), NFKB (Vaiman *et al.*, 2013), EBF1 (Buckberry *et al.*, 2017), RELA (Minekawa *et al.*, 2007), and RORA (Qiu *et al.*, 2015) are implicated in placental development/disease; NFYA (Jin *et al.*, 2001), NFKB (Puscheck *et al.*, 2015), and RELA (Yamamoto *et al.*, 2017) are associated with environmental-induced stressors. These analyses suggested that BDE-47 exposure may impact specific transcriptional responses of CTBs.

Global CpG Methylation Analysis of BDE-47-Exposed CTBs

In parallel with the transcriptomic analyses, we profiled global CpG methylation in BDE-47 (1 μM) and vehicle-exposed CTBs following a 24 h duration (initiated at 3 h or 15 h post-plating). Using a fixed effects linear model, we identified 758 CpGs as DM CpGs associated with BDE-47 exposure ($p \leq .005$; absolute average $\Delta\beta \geq 0.025$). Overall, exposure significantly increased global CpG methylation (0.8 ± 0.2%; Figure 6A). A further increase was observed when the analysis was constrained to BDE-47 DM CpGs (3.4 ± 0.3%; Figure 6A). This was consistent with data from individual CpGs; 93% had increased methylation (708/758 total) and 7% had decreased methylation (50/758 total; Figure 6B). On average, methylation changes due to BDE-47 were similar whether exposures were initiated at 3 h or 15 h ($y = 0.90x$, $R^2 = 0.69$; Figs. 6A–C).

Furthermore, within the BDE-47 DM CpG subset, we asked whether there was enrichment based on gene features. Intergenic sequences were overrepresented and those proximal

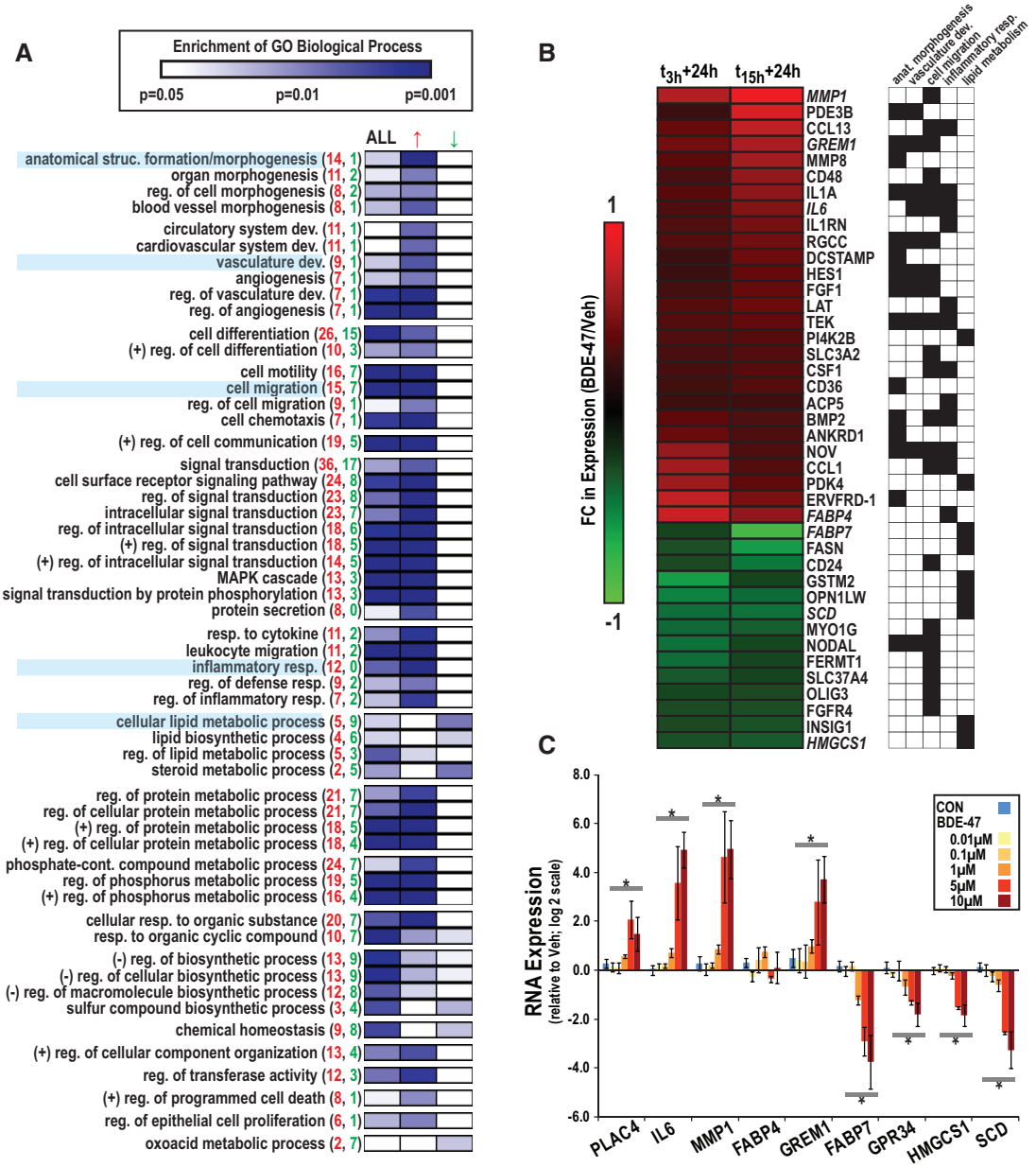

Figure 5. Functional analyses of genes that were DE due to BDE-47 exposures in CTBs. A, Enriched GO Biological Processes within BDE-47 DE Genes identified using DAVID (criteria: $p \leq .01$, number of DE genes associated with enriched term ≥ 7). GO enrichment scores (-log (p)) are displayed for all BDE-47 DE Genes and upregulated or downregulated gene subsets. The total number of DE Genes due to BDE-47 is located in parentheses (up, downregulated). B, Clustering of BDE-47 DE Genes associated with terms: anatomical structure formation involved in morphogenesis, vasculature development, cell migration, inflammatory response, and cellular lipid metabolic process. FC values represent average difference between BDE-47 and vehicle control. C, Concentration-dependent expression alterations in BDE-47 DE Genes using qRT-PCR. Expression values ($-\Delta\Delta CT$) were normalized to housekeeping genes (GAPDH, ACTB) and adjusted by the respective vehicle control. Asterisks indicate significance across all concentrations of BDE-47 and vehicle control (ANOVA, $p < .05$). All targets were observed to be significantly altered, with the exception of FABP4, which was significantly altered only with 1 μM in pairwise comparisons with the vehicle control.

to promoters (eg, TSS1500, TS200, first Exon) were underrepresented (Figure 6D). A relatively large number were also associated with gene bodies, although this feature did not achieve statistical significance because the identified regions did not exceed expectations. GO analyses of genes near BDE-47 DM CpGs revealed enrichment of processes and pathways that are involved in hormone response, cellular projection, signaling, response to oxygen-containing compounds, morphogenesis, and vesicle transport/localization (Figure 6E). Promoter proximal BDE-47 DM CpGs (178 total) were significantly associated with vesicle transport/localization and secretion-related terms.

Next, we examined the chromosomal location of BDE-47 DM CpGs, which on the whole, showed a larger proportion of increased versus decreased methylated CpGs on each chromosome (Figure 7A). The results revealed enrichment on chromosomes 10 and 11 and a relative absence on chromosome 18. Figure 7B shows the chromosome 11 data, which had the highest significance of enrichment, by genomic location. This enabled identification of a BDE-47 DM CpG cluster on Ch. 11p15.5

Table 1. Transcription Factor Binding Site (TFBS) Enrichment Analysis of BDE-47 DE Genes

TF	JASPAR	TFBSs	Z	Genes	Fisher	Count (pct.)	Age, FC (Second /Term)
NFYA	MA0060.1	45	16.6	30 (16↑, 14↓)	3.4	73%	−0.07
AR	MA0007.1	3	10.8	3 (3↑, 0↓)	2.4	33%	−0.46
PBX1	MA0070.1	18	10.7	17 (12↑, 5↓)	4.9	85%	1.19**
EBF1	MA0154.1	94	10.6	52 (36↑, 16↓)	4.2	35%	−0.27
RORA (1)	MA0071.1	43	10.2	26 (17↑, 9↓)	1.4	47%	1.68**
GFI	MA0038.1	126	9.7	59 (37↑, 22↓)	3.4	13%	0.36
TBP	MA0108.2	64	9.0	34 (22↑, 12↓)	1.0	56%	0.07
NFKB	MA0061.1	48	7.8	29 (17↑, 12↓)	1.0	85%	0.36*
RELA	MA0107.1	35	7.5	25 (18↑, 7↓)	1.6	88%	−0.13
TCFCP2L1	MA0145.1	71	7.0	40 (28↑, 12↓)	1.2	89%	1.64**

Overrepresented motifs and associated transcription factors (TFs) in proximity of genes DE by BDE-47 in CTBs. Number of DE genes (up vs downregulated) with TF-binding sites are displayed in combination with corresponding enrichment values for TF binding sites (Z) and genes (Fisher). Abundance of RNA levels (percentile in top 20 000 genes) of TFs in freshly isolated second trimester and term CTBs as determined via post-hoc analysis of RNA-seq data. Significance of differences in expression between second trimester and term CTBs (*$p < .05$; **$p < .001$).

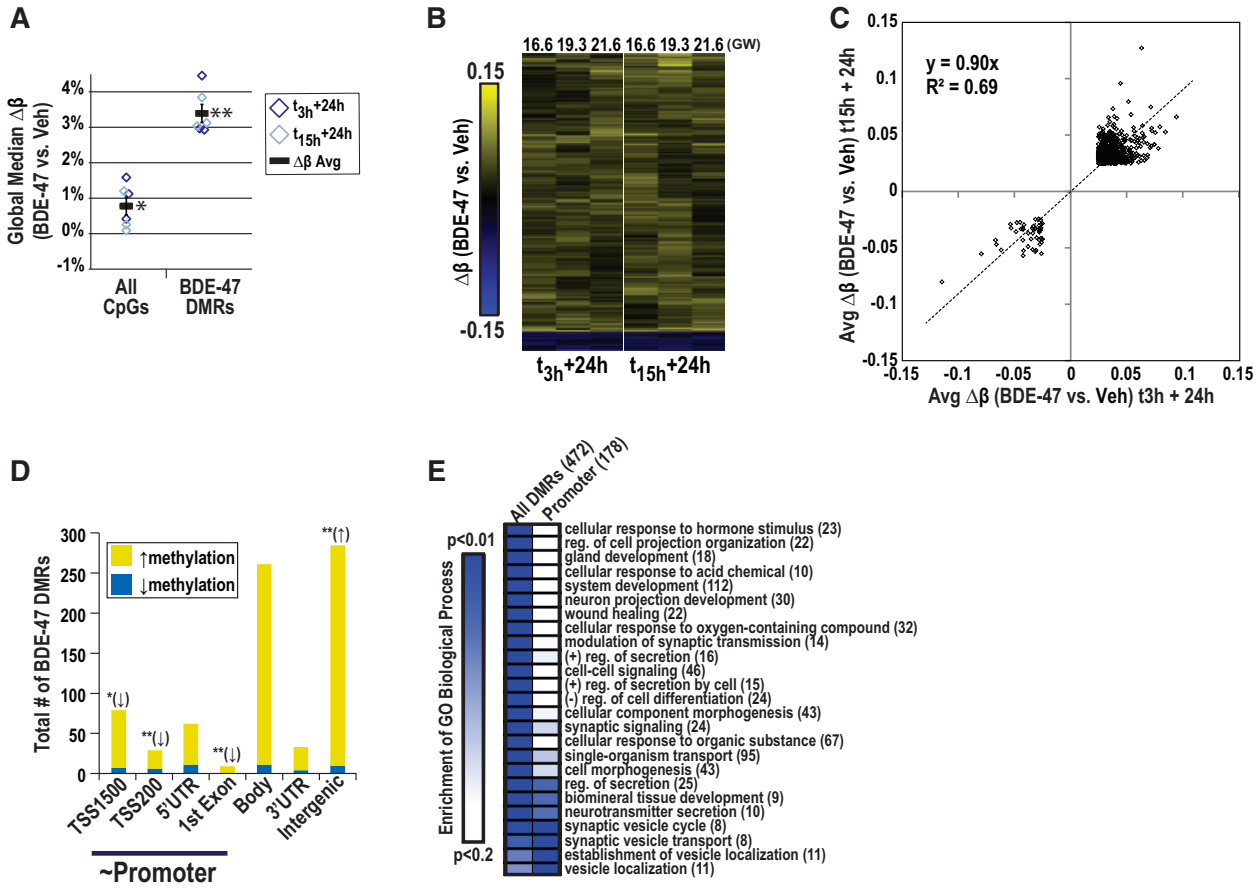

Figure 6. Profiling CpG methylation of BDE-47-exposed CTBs. Cultured CTBs were exposed to 1 μM BDE-47 or 0.1% DMSO for 24 h (initiated at 3 or 15 h post-plating). We identified 758 CpGs to be DM with BDE-47 versus 0.1% DMSO ($p \leq .005$; absolute average $\Delta\beta \geq 0.025$). A, Median difference in methylation levels ($\Delta\beta$) between BDE-47 exposed and vehicle control cultures in all evaluated CpGs and BDE-47 DM CpGs after 24 h. B, Hierarchical clustering of the changes in methylation in BDE-47 DM CpGs (BDE-47 vs concurrent vehicle control). C, Cross-scatter plot comparing average $\Delta\beta$ in BDE-47 response in CTBs exposed at $t_{3\ h}$ or $t_{15\ h} + 24$ h. D, Distribution of BDE-47 DM CpGs by regulatory region. Asterisks indicate over (↑) or under (↓) representation (Fisher's test; (*) $p \leq .05$, (**) $p \leq .001$)). E, Enrichment of GO biological processes within genes (# in parentheses) in proximity of BDE-47 DM CpGs.

(see arrow marked with an asterisk; genome location: 2000000–2300000). Interestingly, the mRNAs encoded by genes in this region (*H19*, *IGF2*, *INS-IGF2*, and *ASCL2*), whose products are among the most abundant in CTBs, play a critical role in gestational development (Smith *et al.*, 2007) and are responsive to multiple environmental exposures (LaRocca *et al.*, 2014; Wu *et al.*, 2004).

Correlating BDE-47-Induced Changes in DNA Methylation With Alterations at the mRNA Level

We identified 178 DM CpGs in gene promoters. A subset (156 of which 152 were unique) were correlated with mRNA expression levels. In total, four genes (3 unique mRNAs) whose promoters were DM had mRNA levels that were also responsive to BDE-47

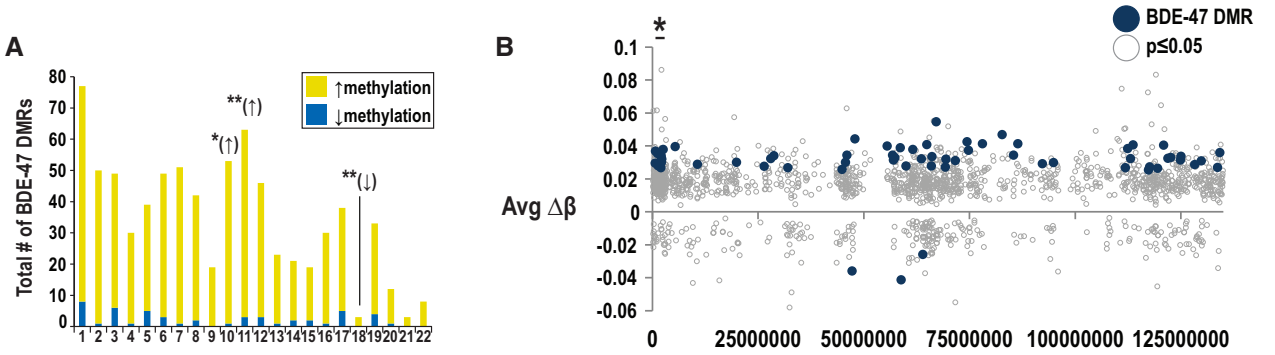

Figure 7. Chromosomal distribution of dysmethylated CpGs in BDE-47-exposed CTBs. A, Location of BDE-47 DM CpGs by chromosome. Asterisks indicate over (↑) or under (↓) representation (Fisher's test; $^{*}p \leq .05$, $^{**}p \leq .001$). B, Change in methylation ($\Delta\beta$) between BDE-47 exposed and vehicle control in CpGs across chromosome 11. Dark blue and gray dots signify significant BDE-47 DM CpGs and CpGs with $p \leq .05$, respectively. Asterisk indicates cluster of BDE-47 DM CpGs located in Ch. 11p15.5.

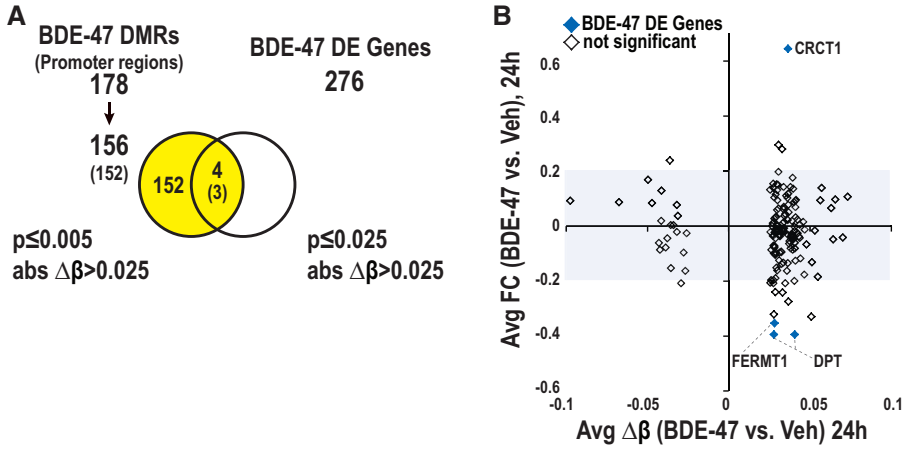

Figure 8. Correlation between BDE-47 altered methylated promoter regions and gene expression. A, The overlap of BDE-47 DM CpGs (associated genes located in promoter regions of DM CpGs) and BDE-47 DE Genes. B, Correlation of average FC in gene expression (*y*-axis) and Δβ (*x*-axis) associated with BDE-47 exposures in gene subset (shaded in Venn). DE Genes are shown as solid blue diamonds.

(Figure 8A). We plotted the average Δβ versus the average FC in expression between BDE-47 and vehicle control for the entire subset (Figure 8B). We identified three mRNA targets of BDE-47 (FERMT1, DPT; downregulated; CRCT1 upregulated) with increased CpG methylation in their promoters due to chemical exposure (Solid blue diamonds, quadrant IV). Our results suggest that BDE-47 exposures may alter the expression of specific genes by modifying CpG methylation within promoter regions.

DISCUSSION

Due to widespread identification of PBDEs in human placental tissues (Leonetti *et al.*, 2016; Zota *et al.*, 2018) and increasing evidence that these compounds cause placental toxicity in rodent and human cell lines (park and Loch-Caruso, 2014, 2015), we utilized a primary cell model to evaluate the effects of BDEs on human CTB differentiation. First, we surveyed a wide range of BDE-47 and -99 concentrations (0.1–25 μM) for cytotoxicity (Figure 1). Both congeners induced significant concentration-dependent effects on cell viability and death. CTBs displayed sensitivities in the range of other vulnerable human cells, eg, primary fetal human neural progenitor cells (Schreiber *et al.*, 2010). Furthermore, PBDEs were more potent in inducing cytotoxicity as compared to other common endocrine disruptors, BPA or PFOA, suggesting PBDEs are relatively potent toxicants in the CTB model.

In CTBs exposed to subcytotoxic concentrations of BDE-47 (Figure 2), we demonstrated acute cellular bioaccumulation of the unmetabolized form after 24 h. These results agree with previous toxicological studies in rodent *in vitro* or *in vivo* models that described cellular/tissue accumulation of PBDEs (Mundy *et al.*, 2004). Partitioning of BDE-47 between the media and cellular fractions was dependent on the initial testing concentration, with a greater proportion of BDE-47 distributed in the cells exposed to 5 μM versus 1 μM. This provided a possible basis for concentration-dependent, nonlinear responses to BDE-47 on the mRNA level. We did not detect a significant amount of the major hydroxylated metabolites of BDE-47 (5-OH or 6-OH). This finding and the observation that ~100% of the parent compound was recovered in the cell/media fractions suggested limited metabolism over 24 h. While the placenta may act as a barrier for several xenobiotics (Robins *et al.*, 2011), its capacity to metabolize PBDEs remains unknown. Other studies from our laboratory (Roadmap Epigenomics *et al.*, 2015) and other groups (Hakkola *et al.*, 1996), indicate that CYP2B6-the primary CYP p450 enzyme involved in BDE-47 metabolism (Feo *et al.*, 2013; Penell *et al.*, 2014)-is expressed at low levels in the placenta.

Here, we present data suggesting that CTBs are unable to breakdown BDE-47 *in vitro*. These mass spectrometry analyzes showed that other primary PBDE congeners (~0.4%) were also present in the mixture. Even though these co-contaminants were a minor component, they could contribute to the observed downstream effects. Future studies are needed to address whether CTB accumulation of PBDEs depends on the exposure duration (acute vs chronic) and the contribution of other placental cell types, eg, STBs, to the metabolism of these compounds.

We tested the ability of BDE-47 to alter CTB migration or invasion—inherent properties of CTBs that enable successful penetration of the decidua and the resident blood vessels. Furthermore, perturbations in CTB migration/invasion underlie pregnancy complications such as PE, PTL, and IUGR, contributing to the pathogenesis of adverse neonatal outcomes (Kaufmann *et al.*, 2003). Our results suggest that BDE-47 significantly disrupts the ability of CTBs to migrate and invade (Figure 3) in line with studies indicating other toxicological compounds, eg, arsenic (Li, and Loch-Caruso, 2007), cadmium (Alvarez, and Chakraborty 2011), impair trophoblast migration. Together these results provide a potential link between chemical exposures, trophoblast dysfunction, and placental-driven pregnancy complications.

Additionally, we conducted a comprehensive assessment of transcriptomic and methylomic changes which correlate with BDE-47 exposure in CTBs. We observed that a subcytotoxic concentration (1 μM) of BDE-47 induces perturbations on transcriptomic and methylomic levels in cultured CTBs isolated from three independent human placentas. We profiled the effects of BDE-47 following a 24 h exposure duration, which was either initiated at $t_{3\ h}$ and $t_{15\ h}$, corresponding with the (1) initial projection of CTB migration or (2) CTB aggregation, respectively (Robinson *et al.*, 2017). In general, significant genomic responses to BDE-47 were similar, irrespective of when exposures were introduced into the media. Overall, these results suggest a general conservation of BDE-47 response in our model system. Future studies which employ larger sample sizes will enable interrogation of factors which also may play a role in sensitivity to environmental exposures *in utero* such as sex, ethnicity, and maternal and gestational age.

As for effects on the transcriptome, we observed dysregulated expression of 276 genes with BDE-47 exposure (Figure 4). Our analyses highlight DE genes associated with (1) proposed mechanisms of PBDE-toxicity, eg, inflammation, Δ hormone response; and (2) pathways critical for placental and trophoblast development. Below, we discuss specific targets of BDE-47 in CTBs that were identified in this study, and their proposed roles in placental development and disease.

Interleukins and other inflammatory mediators drive signaling aspects of placental development and hyperexpression may signal or contribute to pregnancy complications (Tjoa *et al.*, 2003). Here, we provide evidence that BDE-47 alters the expression of several genes known to regulate inflammatory response (Figure 5). Genes dysregulated by BDE-47, included: IL-6 (↑), IL1A (↑), IL1RN (↑), CCL1 (↑), and CCL13 (↑). Interestingly, IL6 may play major roles in immune defense (Rose-John *et al.*, 2017), and altered expression may underlie placental (Prins *et al.*, 2012) and neurodevelopmental disease (Shen *et al.*, 2008; Sorokin *et al.*, 2014). Supporting these findings, in a human trophoblast cell line, in a concentration and time-dependent manner, BDE-47 co-induced IL-6, IL-8, and oxidative stress mediators (park and Loch-Caruso, 2014, 2015). Our results support the hypothesis that PBDE exposures cause inflammation in the placenta, which may contribute to toxicity.

Due to their inherent lipophilic properties and similarities in biochemistry as endogenous hormones, PBDEs and other EDCs may alter cholesterol and fatty acid metabolism pathways which influence the regulation/production of critical hormones for fetal growth. In rodent models, PBDE exposure leads to disruption of specific hormones in placenta (Zhu *et al.*, 2017a) and Leydig cells (Zhao *et al.*, 2011) as well as increased cholesterol serum levels in perinatally exposed juveniles (Tung *et al.*, 2017). Here, we propose specific mRNA targets such as regulatory binding proteins (FABP7 [Thumser *et al.*, 2014], INSIG1 [Dong, and Tang, 2010]) and metabolizing enzymes (FASN [Jones, and Infante, 2015], HMGCS1 [Vock *et al.*, 2008], SCD [Zhang *et al.*, 2005]) involved in lipid/cholesterol metabolism to be significantly downregulated with BDE-47. While these pathways during fetal development are clearly important, the specific role of these molecules in the context of chemical toxicity and/or trophoblast differentiation remains undefined. Our results suggest BDE-47 alters the expression of molecules regulating cholesterol/fatty acid biosynthesis, which may play upstream roles in hormonal regulation in the placenta.

We observed several molecules with known critical functions in placental development, including: (1) maintenance of trophoblast progenitor populations, eg, BMP2 (↑, [Golos *et al.*, 2013]) and NODAL (↓, [Ma *et al.*, 2001]); (2) trophoblast invasion, eg, MMP1 (↑, [Cohen *et al.*, 2006]), MMP8 (↑, [Zhu *et al.*, 2012]); and (3) villi morphogenesis, eg, GREM1 (↑, [O'Connell *et al.*, 2013]), to be significantly altered by BDE-47 exposures (Figure 5B). In addition, our analyzes revealed targets with less defined roles in placentation with links with placental complications, eg, PLAC4 (↑, (Tuohey *et al.*, 2013]), and candidates yet to be studied in the context of placental development. For example, BDE-47-induced expression of GPR34 (Figure 5C), which controls aspects of migration in cancer cells (Jin *et al.*, 2015), and may be required for sufficient immune response to pathogens (Liebscher *et al.*, 2011). Our findings, which complement our observations of BDE-47 functional impairment, provide specific pathways with known roles in trophoblast/placental development to be significantly altered with exposure.

We evaluated for potential upstream regulators of BDE-47 DE Genes by conducting enrichment analysis of TF-related motifs in promoter regions of the gene subset (**Table 1**). In previous studies, similar approaches have been applied to propose key regulatory nodes of developmental toxicity (Robinson *et al.*, 2011). Based on these analyses, we identified TFs involved in PBDE-induced response such as NFKB, a highly recognized TF involved in regulating inflammation signaling pathways in the placenta, and environmental stress-responsive gene expression networks (Simmons *et al.*, 2009). Interestingly, other TFs identified through this analysis, eg, RORA (Qiu *et al.*, 2015), RELA (Minekawa *et al.*, 2007), were also found to differ in expression levels between second trimester and term CTBs and have postulated roles in placenta development, suggesting that these TFs may regulate PBDE-response networks in the context of altered trophoblast development.

While the mechanisms remain poorly understood, diverse environmental exposures, including PBDEs (Byun *et al.*, 2015; Kappil *et al.*, 2016; Sales, and Joca, 2016; Woods *et al.*, 2012), are associated with epigenetic modifications which may regulate transient or irreversible genomic changes leading to transgenerational inheritance of altered phenotypes (Bernal, and Jirtle, 2010; Skinner, and Guerrero-Bosagna, 2009). Here, in parallel with transcriptomic assessments, we provide evidence of BDE-47 exposures to produce subtle, but significant, global changes on the methylome following a 24 h exposure duration (Figs. 6

and 7). Within the subset of BDE-47 DM CpGs, the majority of CpG sites were increased in methylation with BDE-47 (average $\Delta\beta = 3.4\%\uparrow$; 93% CpGs were increased, $\beta > 0$), and predominately located in nonpromoter regions (ie, intergenic positions, gene body). Interestingly, in general, these observations did not correlate with a global reduction in transcription (Figure 8) or modified expression of DNA methyltransferases (DNMTs)/TET family enzyme members (not shown). *In vitro*, upon plating, proliferating CTBs exit the cell cycle, and do not propagate in culture. At each autosomal CpG site, methylation is expected to be 0, 50, or 100% methylated. Thus, the subtle changes in methylation observed with BDE-47 may represent an active binary shift (methylated vs not methylated) in a subset of cells in culture. While increased DNA methylation within promoter regions is a recognized mechanism in silencing mRNA transcription, the role of methylation within nonpromoter regions remains undefined and complex (Szyf, 2011). For instance, increased global methylation within gene-body regions may actually promote gene expression by suppressing cryptic promoters, eg, antisense targets, which compete with RNA Polymerase II-directed transcription (Gagnon-Kugler *et al.*, 2009). Furthermore, global changes in methylation due to environmental exposures are of particular interest in the context of the placenta due to its unique DNA methylation and chromatin state. As compared with adult somatic cells and tissues, the CTB and placental genome is (1) globally hypomethylated; (2) contains a higher proportion of variably methylated CpG sites (β = 20–80% methylated); and (3) age-dependent in its specificity (global methylation higher at term versus second trimester [Roadmap Epigenomics *et al.*, 2015]). Therefore, our results which suggest environmental-induced changes on a global methylation level could have dramatic long-term impact(s) on regulatory molecular/cellular functions of the dynamically changing placenta.

Examining the localized distribution of DM CpGs across the genome, we identified a vulnerable region located on Ch. 11p15.5, which included five DM CpGs (all ↑) due to BDE-47 exposure (Figure 7B, asterisk). This region of Ch. 11 has previously been identified to contain a cluster of imprinted genes important for fetal growth, which have significant associations with several gestational diseases (Smith *et al.*, 2007). Interestingly, genes within this cluster, H19, IGF2, and INS-IGF2, are in the top 99% of abundant transcripts in trophoblast cell populations based on analyzes of second and term trophoblasts in our laboratory (not shown), further suggesting a high level of importance of these molecules in CTB development. Recently, investigators have summarized growing evidence linking alterations in genomic imprinting of this region and adverse placental, ie, PE, and neurobehavioral disease outcomes (Nomura *et al.*, 2017)-key outcomes of interest in regards to PBDEs and other chemical exposures which occur during human pregnancy. Our study along with other environmental investigations in rodent (Ouko *et al.*, 2009; Susiarjo *et al.*, 2013; Wu *et al.*, 2004) and humans (LaRocca *et al.*, 2014) suggest associations between environmental exposures and epigenetic alterations within this particular gene cluster to have high sensitivity and importance in developmental toxicology.

Limited overlap in genes linked with BDE-47 DM CpGs (located in promoter regions) and BDE-47 DE Genes were identified (4 total, 3 unique genes; Figure 8). Closer examination of the influence of BDE-47 on methylation within DM CpGs and RNA expression, in general, suggests a lack of correlation between Δ in methylation and expression due to BDE-47 at 24 h. Poor correlation could be due to the lack of temporal data. Our comparative analyses indicate that two candidates may be epigenetically controlled in response to BDE-47. Both targets, DPT and FERMT1, were identified to have increased methylation in the promoter region associated with downregulation of expression with BDE-47 exposure. These molecules have relatively unknown functions in placentation, but recent evidence implies roles in adhesion and cell migration (Liu *et al.*, 2013) as well as links to regulatory pathways known to be important for trophoblast development (DPT: TFG-β signaling [Jones *et al.*, 2006; Okamoto *et al.*, 1999]); FERMT1: epithelial-mesenchymal transition/Wnt-signaling (Knofler, and Pollheimer, 2013; Liu *et al.*, 2017). Future mechanistic studies may explore the relationships between methylation, RNA expression, and impaired outcomes in CTBs as related to BDE-47 exposures.

We tested 0.01–25 μM of BDE-47, which includes concentrations proposed as physiologically relevant for human exposures and which cause deleterious effects in human embryonic/fetal cells (Park *et al.*, 2014; Schreiber *et al.*, 2010). In general, toxicological responses to BDE-47 were observed at concentrations of $\geq$ 1 μM or higher which are ~3 orders of magnitude higher than the geometric mean concentrations (±standard deviation) recently reported in maternal serum (0.17 ± 1.97 ng/g), cord serum (0.22 ± 1.75 ng/g), or placenta (0.15 ± 1.96 ng/g) (Zota *et al.*, 2018). However, extrapolating exposure levels between *in vitro* and *in utero* is challenging due to the numerous factors that influence sensitivity, including: (1) absorption, metabolism, and excretion; (2) length of exposure (chronic vs acute); (3) life-style factors; (4) nutritional status; and (5) life-stage (Doucet *et al.*, 2009; Grandjean, 1992), which are not addressed in cell culture models. Accounting for factors that underlie variable exposures as well as the lipid content of the placenta, *in vitro* concentrations as high as 8 μM are estimated to be relevant to human exposures (Park *et al.*, 2014). Furthermore, during pregnancy, the fetal/placental unit is exposed to multiple PBDEs and other environmental compounds that may act through similar mechanisms, additively or synergistically (Eriksson *et al.*, 2006; Tagliaferri *et al.*, 2010). Future experiments could use the CTB model to evaluate developmental toxicity in the context of other FRs, including emerging alternatives and complex chemical mixtures.

In this study, we demonstrate the application of a primary human villous CTB model to examine potential environmental interactions which occur during placentation using PBDEs as a relevant model chemical toxicant. Primary human placental cells offer multiple advantages as a toxicological model as compared with transformed human cell lines (Bilban *et al.*, 2010) or rodent (Silva, and Serakides, 2016) due to suspected differences in the underlying cellular and molecular components that regulate placental development. Moving forward, larger sample sizes may be incorporated to improve detection of environmental interactions and control for genetic diversity, gestational age, and sex. Future investigations may also add complimentary investigations of other placental cell types, eg, STBs, which may improve resolution of mechanisms proposed to play roles, eg, Δ hormone levels, (Zhu *et al.*, 2017a,b), in PBDE-induced placental toxicity in studies examining the complete placental unit. In summary, we provide evidence that PBDEs induce toxicity in human primary placental cells and alter levels of expression of specific transcripts and epigenetically controlled regions. Perturbations may be evaluated as biomarkers *in vitro* or *in vivo* to determine correlations between PBDEs and adverse developmental/pregnancy outcomes.

SUPPLEMENTARY DATA

Supplementary data are available at *Toxicological Sciences* online.

ACKNOWLEDGMENTS

The authors would like to thank Sirirak Buarpung, Elaine Kwan, Jason Farrell, and Nicomedes Abello for additional technical support; and Michael McMaster and Matthew Gormley for their valuable insight in human placental and trophoblast biology. Tissue samples were provided by the NIH Placental Bank at UCSF, funded under NICHD/NIH Eunice Kennedy Shriver National Institute of Child Health & Human Development of the National Institutes of Health under Award P50HD055764 (to S.J.F.). The authors have nothing to disclose.

FUNDING

This work was kindly supported by the United States Environmental Protection Agency (RD883467801) and the National Institute of Environmental Health Sciences (P01ES022841, R00ES023846).

REFERENCES

Alvarez, M. M., and Chakraborty, C. (2011). Cadmium inhibits motility factor-dependent migration of human trophoblast cells. *Toxicol. In Vitro* **25**(8), 1926–1933.

Arenas-Hernandez, M., and Vega-Sanchez, R. (2013). Housekeeping gene expression stability in reproductive tissues after mitogen stimulation. *BMC Res. Notes* **6**, 285.

Bernal, A. J., and Jirtle, R. L. (2010). Epigenomic disruption: The effects of early developmental exposures. *Birth Defects Res. A Clin. Mol. Teratol.* **88**(10), 938–944.

Bilban, M., Tauber, S., Haslinger, P., Pollheimer, J., Saleh, L., Pehamberger, H., Wagner, O., and Knofler, M. (2010). Trophoblast invasion: Assessment of cellular models using gene expression signatures. *Placenta* **31**, 989–996.

Borenfreund, E., and Puerner, J. A. (1985). Toxicity determined in vitro by morphological alterations and neutral red absorption. *Toxicol. Lett.* **24**(2-3), 119–124.

Buckberry, S., Bianco-Miotto, T., Bent, S. J., Clifton, V., Shoubridge, C., Shankar, K., and Roberts, C. T. (2017). Placental transcriptome co-expression analysis reveals conserved regulatory programs across gestation. *BMC Genomics* **18**, 10.

Burton, G. J., Fowden, A. L., and Thornburg, K. L. (2016). Placental origins of chronic disease. *Physiol. Rev.* **96**, 1509–1565.

Byun, H. M., Benachour, N., Zalko, D., Frisardi, M. C., Colicino, E., Takser, L., and Baccarelli, A. A. (2015). Epigenetic effects of low perinatal doses of flame retardant BDE-47 on mitochondrial and nuclear genes in rat offspring. *Toxicology* **328**, 152–159.

Chen, Z., Liu, J., Ng, H. K., Nadarajah, S., Kaufman, H. L., Yang, J. Y., and Deng, Y. (2011). Statistical methods on detecting differentially expressed genes for RNA-seq data. *BMC Syst. Biol.* **5**, S1.

Cohen, M., Meisser, A., and Bischof, P. (2006). Metalloproteinases and human placental invasiveness. *Placenta* **27**, 783–793.

Costa, L. G., de Laat, R., Tagliaferri, S., and Pellacani, C. (2014). A mechanistic view of polybrominated diphenyl ether (PBDE) developmental neurotoxicity. *Toxicol. Lett.* **230**, 282–294.

Costa, L. G., Pellacani, C., Dao, K., Kavanagh, T. J., and Roque, P. J. (2015). The brominated flame retardant BDE-47 causes oxidative stress and apoptotic cell death in vitro and in vivo in mice. *Neurotoxicology* **48**, 68–76.

Cowell, W. J., Lederman, S. A., Sjodin, A., Jones, R., Wang, S., Perera, F. P., Wang, R., Rauh, V. A., and Herbstman, J. B. (2015). Prenatal exposure to polybrominated diphenyl ethers and child attention problems at 3-7 years. *Neurotoxicol. Teratol.* **52**, 143–150.

Damsky, C. H., Fitzgerald, M. L., and Fisher, S. J. (1992). Distribution patterns of extracellular matrix components and adhesion receptors are intricately modulated during first trimester cytotrophoblast differentiation along the invasive pathway, in vivo. *J. Clin. Invest.* **89**, 210–222.

Dingemans, M. M., van den Berg, M., and Westerink, R. H. (2011). Neurotoxicity of brominated flame retardants: (in)direct effects of parent and hydroxylated polybrominated diphenyl ethers on the (developing) nervous system. *Environ. Health Perspect.* **119**, 900–907.

Dong, X. Y., and Tang, S. Q. (2010). Insulin-induced gene: A new regulator in lipid metabolism. *Peptides* **31**(11), 2145–2150.

Doucet, J., Tague, B., Arnold, D. L., Cooke, G. M., Hayward, S., and Goodyer, C. G. (2009). Persistent organic pollutant residues in human fetal liver and placenta from Greater Montreal, Quebec: A longitudinal study from 1998 through 2006. *Environ. Health Perspect.* **117**, 605–610.

Du, P., Zhang, X., Huang, C. C., Jafari, N., Kibbe, W. A., Hou, L., and Lin, S. M. (2010). Comparison of Beta-value and M-value methods for quantifying methylation levels by microarray analysis. *BMC Bioinformatics* **11**, 587.

Eriksson, P., Fischer, C., and Fredriksson, A. (2006). Polybrominated diphenyl ethers, a group of brominated flame retardants, can interact with polychlorinated biphenyls in enhancing developmental neurobehavioral defects. *Toxicol. Sci.* **94**, 302–309.

Feo, M. L., Gross, M. S., McGarrigle, B. P., Eljarrat, E., Barcelo, D., Aga, D. S., and Olson, J. R. (2013). Biotransformation of BDE-47 to potentially toxic metabolites is predominantly mediated by human CYP2B6. *Environ. Health Perspect.* **121**(4), 440–446.

Fisher, S. J. (2015). Why is placentation abnormal in preeclampsia? *Am. J. Obstet. Gynecol.* **213**, S115–S122.

Fisher, S. J., Cui, T. Y., Zhang, L., Hartman, L., Grahl, K., Zhang, G. Y., Tarpey, J., and Damsky, C. H. (1989). Adhesive and degradative properties of human placental cytotrophoblast cells in vitro. *J. Cell Biol.* **109**, 891–902.

Frederiksen, M., Vorkamp, K., Thomsen, M., and Knudsen, L. E. (2009). Human internal and external exposure to PBDEs - A review of levels and sources. *Int. J. Hyg. Environ. Health* **212**, 109–134.

Gagnon-Kugler, T., Langlois, F., Stefanovsky, V., Lessard, F., and Moss, T. (2009). Loss of human ribosomal gene CpG methylation enhances cryptic RNA polymerase II transcription and disrupts ribosomal RNA processing. *Mol. Cell* **35**, 414–425.

Gene Ontology Consortium. (2015). Gene Ontology Consortium: Going forward. *Nucleic Acids Res.* **43**, D1049–D1056.

Giraldo, J., Vivas, N. M., Vila, E., and Badia, A. (2002). Assessing the (a)symmetry of concentration-effect curves: Empirical versus mechanistic models. *Pharmacol. Ther.* **95**, 21–45.

Golos, T. G., Giakoumopoulos, M., and Gerami-Naini, B. (2013). Review: Trophoblast differentiation from human embryonic stem cells. *Placenta* **34**, S56–S61.

Grandjean, P. (1992). Individual susceptibility to toxicity. *Toxicol. Lett.* **64-65**, 43–51.

Hakkola, J., Pasanen, M., Hukkanen, J., Pelkonen, O., Maenpaa, J., Edwards, R. J., Boobis, A. R., and Raunio, H. (1996). Expression of xenobiotic-metabolizing cytochrome P450 forms in human full-term placenta. *Biochem. Pharmacol.* **51**, 403–411.

Herbstman, J. B., and Mall, J. K. (2014). Developmental exposure to polybrominated diphenyl ethers and neurodevelopment. *Curr. Environ. Health Rep.* **1**(2), 101–112.

Hromatka, B. S., Drake, P. M., Kapidzic, M., Stolp, H., Goldfien, G. A., Shih Ie, M., and Fisher, S. J. (2013). Polysialic acid enhances the migration and invasion of human cytotrophoblasts. *Glycobiology* **23**, 593–602.

Huang, D. W., Sherman, B. T., Tan, Q., Collins, J. R., Alvord, W. G., Roayaei, J., Stephens, R., Baseler, M. W., Lane, H. C., and Lempicki, R. A. (2007). The DAVID Gene Functional Classification Tool: A novel biological module-centric algorithm to functionally analyze large gene lists. *Genome Biol.* **8**, R183.

Hunkapiller, N. M., and Fisher, S. J. (2008). Chapter 12. Placental remodeling of the uterine vasculature. *Methods Enzymol.* **445**, 281–302.

Jauniaux, E., and Jurkovic, D. (2012). Placenta accreta: Pathogenesis of a 20th century iatrogenic uterine disease. *Placenta* **33**(4), 244–251.

Jin, S., Fan, F., Fan, W., Zhao, H., Tong, T., Blanck, P., Alomo, I., Rajasekaran, B., and Zhan, Q. (2001). Transcription factors Oct-1 and NF-YA regulate the p53-independent induction of the GADD45 following DNA damage. *Oncogene* **20**, 2683–2690.

Jinhui, L., Yuan, C., and Wenjing, X. (2015). Polybrominated diphenyl ethers in articles: A review of its applications and legislation. *Environ. Sci. Pollut. Res. Int.* doi: 10.1007/s11356-015-4515-6.

Jin, Z. T., Li, K., Li, M., Ren, Z. G., Wang, F. S., Zhu, J. Y., Leng, X. S., and Yu, W. D. (2015). G-protein coupled receptor 34 knockdown impairs the proliferation and migration of HGC-27 gastric cancer cells in vitro. *Chin. Med. J.* **128**, 545–549.

Jones, S. F., and Infante, J. R. (2015). Molecular pathways: Fatty acid synthase. *Clin. Cancer Res.* **21**(24), 5434–5438.

Jones, R. L., Stoikos, C., Findlay, J. K., and Salamonsen, L. A. (2006). TGF-beta superfamily expression and actions in the endometrium and placenta. *Reproduction* **132**, 217–232.

Kalkunte, S., Huang, Z., Lippe, E., Kumar, S., Robertson, L. W., and Sharma, S. (2017). Polychlorinated biphenyls target Notch/Dll and VEGF R2 in the mouse placenta and human trophoblast cell lines for their anti-angiogenic effects. *Sci. Rep.* **7**, 39885.

Kappil, M. A., Li, Q., Li, A., Dassanayake, P. S., Xia, Y., Nanes, J. A., Landrigan, P. J., Stodgell, C. J., Aagaard, K. M., Schadt, E. E., *et al.* (2016). In utero exposures to environmental organic pollutants disrupt epigenetic marks linked to fetoplacental development. *Environ. Epigenet.* **2**, dvv013.

Kaufmann, P., Black, S., and Huppertz, B. (2003). Endovascular trophoblast invasion: Implications for the pathogenesis of intrauterine growth retardation and preeclampsia. *Biol. Reprod.* **69**, 1–7.

Kliman, H. J., Nestler, J. E., Sermasi, E., Sanger, J. M., and Strauss, J. F. (1986). Purification, characterization, and in vitro differentiation of cytotrophoblasts from human term placentae. *Endocrinology* **118**, 1567–1582.

Knofler, M., and Pollheimer, J. (2013). Human placental trophoblast invasion and differentiation: A particular focus on Wnt signaling. *Front. Genet.* **4**, 190.

Kovo, M., Schreiber, L., Ben-Haroush, A., Gold, E., Golan, A., and Bar, J. (2012). The placental component in early-onset and late-onset preeclampsia in relation to fetal growth restriction. *Prenat. Diagn.* **32**, 632–637.

LaRocca, J., Binder, A. M., McElrath, T. F., and Michels, K. B. (2014). The impact of first trimester phthalate and phenol exposure on IGF2/H19 genomic imprinting and birth outcomes. *Environ. Res.* **133**, 396–406.

Leonetti, C., Butt, C. M., Hoffman, K., Miranda, M. L., and Stapleton, H. M. (2016). Concentrations of polybrominated diphenyl ethers (PBDEs) and 2, 4, 6-tribromophenol in human placental tissues. *Environ. Int.* **88**, 23–29.

Li, C. S., and Loch, C. R. (2007). Sodium arsenite inhibits migration of extravillous trophoblast cells in vitro. *Reprod. Toxicol.* **24**(3-4), 296–302.

Liebscher, I., Muller, U., Teupser, D., Engemaier, E., Engel, K. M., Ritscher, L., Thor, D., Sangkuhl, K., Ricken, A., Wurm, A., *et al.* (2011). Altered immune response in mice deficient for the G protein-coupled receptor GPR34. *J. Biol. Chem.* **286**, 2101–2110.

Liu, C. C., Cai, D. L., Sun, F., Wu, Z. H., Yue, B., Zhao, S. L., Wu, X. S., Zhang, M., Zhu, X. W., Peng, Z. H., *et al.* (2017). FERMT1 mediates epithelial-mesenchymal transition to promote colon cancer metastasis via modulation of beta-catenin transcriptional activity. *Oncogene* **36**, 1779–1792.

Liu, X., Meng, L., Shi, Q., Liu, S., Cui, C., Hu, S., and Wei, Y. (2013). Dermatopontin promotes adhesion, spreading and migration of cardiac fibroblasts in vitro. *Matrix Biol.* **32**, 23–31.

Ma, G. T., Soloveva, V., Tzeng, S. J., Lowe, L. A., Pfendler, K. C., Iannaccone, P. M., Kuehn, M. R., and Linzer, D. I. (2001). Nodal regulates trophoblast differentiation and placental development. *Dev. Biol.* **236**, 124–135.

Maltepe, E., and Fisher, S. J. (2015). Placenta: The forgotten organ. *Annu. Rev. Cell Dev. Biol.* **31**, 523–552.

Minekawa, R., Sakata, M., Okamoto, Y., Hayashi, M., Isobe, A., Takeda, T., Yamamoto, T., Koyama, M., Ohmichi, M., Tasaka, K., *et al.* (2007). Involvement of RelA-associated inhibitor in regulation of trophoblast differentiation via interaction with transcriptional factor specificity protein-1. *Endocrinology* **148**, 5803–5810.

Mundy, W. R., Freudenrich, T. M., Crofton, K. M., and DeVito, M. J. (2004). Accumulation of PBDE-47 in primary cultures of rat neocortical cells. *Toxicol. Sci.* **82**, 164–169.

Nomura, Y., John, R. M., Janssen, A. B., Davey, C., Finik, J., Buthmann, J., Glover, V., and Lambertini, L. (2017). Neurodevelopmental consequences in offspring of mothers with preeclampsia during pregnancy: Underlying biological mechanism via imprinting genes. *Arch. Gynecol. Obstet.* **295**, 1319–1329.

O'Connell, B. A., Moritz, K. M., Walker, D. W., and Dickinson, H. (2013). Synthetic glucocorticoid dexamethasone inhibits branching morphogenesis in the spiny mouse placenta. *Biol. Reprod.* **88**, 26.

Okamoto, O., Fujiwara, S., Abe, M., and Sato, Y. (1999). Dermatopontin interacts with transforming growth factor beta and enhances its biological activity. *Biochem. J.* **337**, 537–541.

Ouko, L. A., Shantikumar, K., Knezovich, J., Haycock, P., Schnugh, D. J., and Ramsay, M. (2009). Effect of alcohol consumption on CpG methylation in the differentially methylated regions of H19 and IG-DMR in male gametes: Implications for fetal alcohol spectrum disorders. *Alcohol. Clin. Exp. Res.* **33**, 1615–1627.

Park, H. R., Kamau, P. W., and Loch-Caruso, R. (2014). Involvement of reactive oxygen species in brominated diphenyl ether-47-induced inflammatory cytokine release from human extravillous trophoblasts in vitro. *Toxicol. Appl. Pharmacol.* **274**, 283–292.

Park, H. R., and Loch-Caruso, R. (2014). Protective effect of nuclear factor E2-related factor 2 on inflammatory cytokine

response to brominated diphenyl ether-47 in the HTR-8/SVneo human first trimester extravillous trophoblast cell line. *Toxicol. Appl. Pharmacol.* **281**(1), 67–77.

Park, H. R., and Loch-Caruso, R. (2015). Protective effect of (+/-)alpha-tocopherol on brominated diphenyl ether-47-stimulated prostaglandin pathways in human extravillous trophoblasts in vitro. *Toxicol. In Vitro* **29**(7), 1309–1318.

Penell, J., Lind, L., Fall, T., Syvanen, A. C., Axelsson, T., Lundmark, P., Morris, A. P., Lindgren, C., Mahajan, A., Salihovic, S., *et al.* (2014). Genetic variation in the CYP2B6 gene is related to circulating 2, 2′, 4, 4′-tetrabromodiphenyl ether (BDE-47) concentrations: An observational population-based study. *Environ. Health* **13**, 34.

Prins, J. R., Gomez-Lopez, N., and Robertson, S. A. (2012). Interleukin-6 in pregnancy and gestational disorders. *J. Reprod. Immunol.* **95**, 1–14.

Puscheck, E. E., Awonuga, A. O., Yang, Y., Jiang, Z., and Rappolee, D. A. (2015). Molecular biology of the stress response in the early embryo and its stem cells. *Adv. Exp. Med. Biol.* **843**, 77–128.

Qiu, C., Gelaye, B., Denis, M., Tadesse, M. G., Luque Fernandez, M. A., Enquobahrie, D. A., Ananth, C. V., Sanchez, S. E., and Williams, M. A. (2015). Circadian clock-related genetic risk scores and risk of placental abruption. *Placenta* **36**, 1480–1486.

Rajakumar, C., Guan, H., Langlois, D., Cernea, M., and Yang, K. (2015). Bisphenol A disrupts gene expression in human placental trophoblast cells. *Reprod. Toxicol.* **53**, 39–44.

Red-Horse, K., Kapidzic, M., Zhou, Y., Feng, K. T., Singh, H., and Fisher, S. J. (2005). EPHB4 regulates chemokine-evoked trophoblast responses: A mechanism for incorporating the human placenta into the maternal circulation. *Development* **132**, 4097–4106.

Red-Horse, K., Zhou, Y., Genbacev, O., Prakobphol, A., Foulk, R., McMaster, M., and Fisher, S. J. (2004). Trophoblast differentiation during embryo implantation and formation of the maternal-fetal interface. *J. Clin. Invest.* **114**, 744–754.

Roadmap Epigenomics, C., Kundaje, A., Meuleman, W., Ernst, J., Bilenky, M., Yen, A., Heravi-Moussavi, A., Kheradpour, P., Zhang, Z., Wang, J., *et al.* (2015). Integrative analysis of 111 reference human epigenomes. *Nature* **518**, 7539317–7539330.

Robins, J. C., Marsit, C. J., Padbury, J. F., and Sharma, S. S. (2011). Endocrine disruptors, environmental oxygen, epigenetics and pregnancy. *Front. Biosci.* **E3**, 690–700.

Robinson, J. F., Gormley, M. J., and Fisher, S. J. (2016). A genomics-based framework for identifying biomarkers of human neurodevelopmental toxicity. *Reprod. Toxicol.* **60**, 1–10.

Robinson, J. F., Kapidzic, M., Gormley, M., Ona, K., Dent, T., Seifikar, H., Hamilton, E. G., and Fisher, S. J. (2017). Transcriptional dynamics of cultured human villous cytotrophoblasts. *Endocrinology* **158**, 1581–1594.

Robinson, J. F., and Piersma, A. H. (2013). Toxicogenomic approaches in developmental toxicology testing. *Methods Mol. Biol.* **947**, 451–473.

Robinson, J. F., Yu, X., Moreira, E. G., Hong, S., and Faustman, E. M. (2011). Arsenic- and cadmium-induced toxicogenomic response in mouse embryos undergoing neurulation. *Toxicol. Appl. Pharmacol.* **250**, 117–129.

Romero, R., Dey, S. K., and Fisher, S. J. (2014). Preterm labor: One syndrome, many causes. *Science* **345**, 760–765.

Rose-John, S., Winthrop, K., and Calabrese, L. (2017). The role of IL-6 in host defence against infections: Immunobiology and clinical implications. *Nat. Rev. Rheumatol.* **13**, 399–409.

Saeed, A. I., Bhagabati, N. K., Braisted, J. C., Liang, W., Sharov, V., Howe, E. A., Li, J., Thiagarajan, M., White, J. A., and Quackenbush, J. (2006). TM4 microarray software suite. *Methods Enzymol.* **411**, 134–193.

Sales, A. J., and Joca, S. R. (2016). Effects of DNA methylation inhibitors and conventional antidepressants on mice behaviour and brain DNA methylation levels. *Acta Neuropsychiatr.* **28**(1), 11–22.

Schreiber, T., Gassmann, K., Gotz, C., Hubenthal, U., Moors, M., Krause, G., Merk, H. F., Nguyen, N. H., Scanlan, T. S., Abel, J., *et al.* (2010). Polybrominated diphenyl ethers induce developmental neurotoxicity in a human in vitro model: Evidence for endocrine disruption. *Environ. Health Perspect.* **118**, 572–578.

Shen, Q., Li, Z. Q., Sun, Y., Wang, T., Wan, C. L., Li, X. W., Zhao, X. Z., Feng, G. Y., Li, S., St Clair, D., *et al.* (2008). The role of pro-inflammatory factors in mediating the effects on the fetus of prenatal undernutrition: Implications for schizophrenia. *Schizophr. Res.* **99**, 48–55.

Silva, J. F., and Serakides, R. (2016). Intrauterine trophoblast migration: A comparative view of humans and rodents. *Cell Adh. Migr.* **10**(1-2), 88–110.

Simmons, S. O., Fan, C. Y., and Ramabhadran, R. (2009). Cellular stress response pathway system as a sentinel ensemble in toxicological screening. *Toxicol. Sci.* **111**, 202–225.

Simon, R., Lam, A., Li, M. C., Ngan, M., Menenzes, S., and Zhao, Y. (2007). Analysis of gene expression data using BRB-Array Tools. *Cancer Inform.* **3**, 11–17.

Skinner, M. K., and Guerrero-Bosagna, C. (2009). Environmental signals and transgenerational epigenetics. *Epigenomics* **1**(1), 111–117.

Smith, A. C., Choufani, S., Ferreira, J. C., and Weksberg, R. (2007). Growth regulation, imprinted genes, and chromosome 11p15.5. *Pediatr. Res.* **61**, 43R–47R.

Sorokin, Y., Romero, R., Mele, L., Iams, J. D., Peaceman, A. M., Leveno, K. J., Harper, M., Caritis, S. N., Mercer, B. M., Thorp, J. M., *et al.* (2014). Umbilical cord serum interleukin-6, C-reactive protein, and myeloperoxidase concentrations at birth and association with neonatal morbidities and long-term neurodevelopmental outcomes. *Am. J. Perinatol.* **31**, 717–726.

Susiarjo, M., Sasson, I., Mesaros, C., and Bartolomei, M. S. (2013). Bisphenol A exposure disrupts genomic imprinting in the mouse. *PLoS Genet.* **9**, e1003401.

Szyf, M. (2011). The implications of DNA methylation for toxicology: Toward toxicomethylomics, the toxicology of DNA methylation. *Toxicol. Sci.* **120**, 235–255.

Tagliaferri, S., Caglieri, A., Goldoni, M., Pinelli, S., Alinovi, R., Poli, D., Pellacani, C., Giordano, G., Mutti, A., and Costa, L. G. (2010). Low concentrations of the brominated flame retardants BDE-47 and BDE-99 induce synergistic oxidative stress-mediated neurotoxicity in human neuroblastoma cells. *Toxicol. In Vitro* **24**, 116–122.

Thumser, A. E., Moore, J. B., and Plant, N. J. (2014). Fatty acid binding proteins: Tissue-specific functions in health and disease. *Curr. Opin. Clin. Nutr. Metab. Care* **17**, 124–129.

Tjoa, M. L., van Vugt, J. M., Go, A. T., Blankenstein, M. A., Oudejans, C. B., and van Wijk, I. J. (2003). Elevated C-reactive protein levels during first trimester of pregnancy are indicative of preeclampsia and intrauterine growth restriction. *J. Reprod. Immunol.* **59**, 29–37.

Tung, E. W. Y., Kawata, A., Rigden, M., Bowers, W. J., Caldwell, D., Holloway, A. C., Robaire, B., Hales, B. F., and Wade, M. G. (2017). Gestational and lactational exposure to an environmentally-relevant mixture of brominated flame retardants: Effects on neurodevelopment and metabolism. *Birth Defects Res.* **109**, 497–512.

Tuohey, L., Macintire, K., Ye, L., Palmer, K., Skubisz, M., Tong, S., and Kaitu'u-Lino, T. J. (2013). PLAC4 is upregulated in severe early onset preeclampsia and upregulated with syncytialisation but not hypoxia. *Placenta* **34**, 256–260.

Vaiman, D., Calicchio, R., and Miralles, F. (2013). Landscape of transcriptional deregulations in the preeclamptic placenta. *PLoS One* **8**, e65498.

Vinnars, M. T., Nasiell, J., Holmstrom, G., Norman, M., Westgren, M., and Papadogiannakis, N. (2014). Association between placental pathology and neonatal outcome in preeclampsia: A large cohort study. *Hypertens. Pregnancy* **33**, 145–158.

Vock, C., Doring, F., and Nitz, I. (2008). Transcriptional regulation of HMG-CoA synthase and HMG-CoA reductase genes by human ACBP. *Cell. Physiol. Biochem.* **22**, 515–524.

Winn, V. D., Haimov-Kochman, R., Paquet, A. C., Yang, Y. J., Madhusudhan, M. S., Gormley, M., Feng, K. T., Bernlohr, D. A., McDonagh, S., Pereira, L., *et al.* (2007). Gene expression profiling of the human maternal-fetal interface reveals dramatic changes between midgestation and term. *Endocrinology* **148**, 1059–1079.

Woodruff, T. J., Zota, A. R., and Schwartz, J. M. (2011). Environmental chemicals in pregnant women in the United States: NHANES 2003–2004. *Environ. Health Perspect.* **119**, 878–885.

Woods, R., Vallero, R. O., Golub, M. S., Suarez, J. K., Ta, T. A., Yasui, D. H., Chi, L. H., Kostyniak, P. J., Pessah, I. N., Berman, R. F., *et al.* (2012). Long-lived epigenetic interactions between perinatal PBDE exposure and Mecp2308 mutation. *Hum. Mol. Genet.* **21**, 2399–2411.

Wu, Q., Ohsako, S., Ishimura, R., Suzuki, J. S., and Tohyama, C. (2004). Exposure of mouse preimplantation embryos to 2, 3, 7, 8-tetrachlorodibenzo-p-dioxin (TCDD) alters the methylation status of imprinted genes H19 and Igf2. *Biol. Reprod.* **70**, 1790–1797.

Yamamoto, M., Khan, N., Muniroh, M., Motomura, E., Yanagisawa, R., Matsuyama, T., and Vogel, C. F. (2017). Activation of interleukin-6 and -8 expressions by methylmercury in human U937 macrophages involves RelA and p50. *J. Appl. Toxicol.* **37**, 611–620.

Yang, K., Julan, L., Rubio, F., Sharma, A., and Guan, H. (2006). Cadmium reduces 11 beta-hydroxysteroid dehydrogenase type 2 activity and expression in human placental trophoblast cells. *Am. J. Physiol. Endocrinol. Metab.* **290**, E135–E142.

Zhang, S., Yang, Y., and Shi, Y. (2005). Characterization of human SCD2, an oligomeric desaturase with improved stability and enzyme activity by cross-linking in intact cells. *Biochem. J.* **388**, 135–142.

Zhao, Y., Ao, H., Chen, L., Sottas, C. M., Ge, R. S., and Zhang, Y. (2011). Effect of brominated flame retardant BDE-47 on androgen production of adult rat Leydig cells. *Toxicol. Lett.* **205**, 209–214.

Zhu, J. Y., Pang, Z. J., and Yu, Y. H. (2012). Regulation of trophoblast invasion: The role of matrix metalloproteinases. *Rev. Obstet. Gynecol.* **5**, e137–e143.

Zhu, Y., Tan, Y. Q., and Leung, L. K. (2017a). Exposure to 2, 2′, 4, 4′-tetrabromodiphenyl ether at late gestation modulates placental signaling molecules in the mouse model. *Chemosphere* **181**, 289–295.

Zhu, Y., Tan, Y. Q., Wang, C. C., and Leung, L. K. (2017). The flame retardant 2, 2′, 4, 4′-Tetrabromodiphenyl ether enhances the expression of corticotropin-releasing hormone in the placental cell model JEG-3. *Chemosphere* **174**, 499–505.

Zota, A. R., Linderholm, L., Park, J. S., Petreas, M., Guo, T., Privalsky, M. L., Zoeller, R. T., and Woodruff, T. J. (2013). Temporal comparison of PBDEs, OH-PBDEs, PCBs, and OH-PCBs in the serum of second trimester pregnant women recruited from San Francisco General Hospital, California. *Environ. Sci. Technol.* **47**, 11776–11784.

Zota, A. R., Mitro, S. D., Robinson, J. F., Hamilton, E. G., Park, J. S., Parry, E., Zoeller, R. T., and Woodruff, T. J. (2018). Polybrominated diphenyl ethers (PBDEs) and hydroxylated PBDE metabolites (OH-PBDEs) in maternal and fetal tissues, and associations with fetal cytochrome P450 gene expression. *Environ. Int.* **112**, 269–278.

Transcriptional Dynamics of Cultured Human Villous Cytotrophoblasts

Joshua F. Robinson,[1,2,3] Mirhan Kapidzic,[1,2,3] Matthew Gormley,[1,2,3] Katherine Ona,[1,2] Terrence Dent,[1,2] Helia Seifikar,[1,2] Emily G. Hamilton,[1,2] and Susan J. Fisher[1,2,3,4,5,6]

[1]Center for Reproductive Sciences, University of California, San Francisco, California 94143; [2]Department of Obstetrics, Gynecology, and Reproductive Sciences, University of California, San Francisco, California 94143; [3]Eli and Edythe Broad Center for Regeneration Medicine and Stem Cell Research, University of California, San Francisco, California 94143; [4]Division of Maternal Fetal Medicine, University of California, San Francisco, California 94143; [5]Department of Anatomy, University of California, San Francisco, California 94143; and [6]Human Embryonic Stem Cell Program, University of California, San Francisco, California 94143

During human pregnancy, cytotrophoblasts (CTBs) play key roles in uterine invasion, vascular remodeling, and anchoring of the feto-placental unit. Due to the challenges associated with studying human placentation *in utero*, cultured primary villous CTBs are used as a model of the differentiation pathway that leads to invasion of the uterine wall. *In vitro*, CTBs emulate *in vivo* cell behaviors, such as migration, aggregation, and substrate penetration. Although some of the molecular features related to these cell behaviors have been described, the underlying mechanisms, at a global level, remain undefined at midgestation. Thus, in this study, we characterized second-trimester CTB differentiation/invasion *in vitro*, correlating the major morphological transitions with the transcriptional changes that occurred at these steps. After plating on Matrigel as individual cells, CTBs migrated toward each other and formed multicellular aggregates. In parallel, using a microarray approach, we observed differentially expressed (DE) genes across time, which were enriched for numerous functions, including cell migration, vascular remodeling, morphogenesis, cell communication, and inflammatory signaling. DE genes encoded several molecules that we and others previously linked to critical CTB function *in vivo*, suggesting that the novel DE molecules we discovered played important roles. Immunolocalization confirmed that CTBs *in situ* gave a signal for two of the most highly expressed genes *in vitro*. In summary, we characterized, at a global level, the temporal dynamics of primary human CTB gene expression in culture. These data will enable future analyses of various types of *in vitro* perturbations—for example, modeling disease processes and environmental exposures. **(*Endocrinology* 158: 1581–1594, 2017)**

Within the intervillous space of the human placenta, networks of chorionic villi suspended in circulating maternal blood facilitate the vital exchange of nutrients, wastes, and gases between the maternal and embryonic/fetal units (Fig. 1). The villi are covered in two trophoblast layers. The outer layer is composed of multinucleated syncytiotrophoblasts, transport, and hormone-producing cells. Beneath resides a polarized layer of mononuclear cytotrophoblast (CTB) progenitors (2). Depending on location, CTBs differentiate into syncytiotrophoblasts or exit the placenta to anchor the embryo/fetus to the uterus. During the latter process, the cells detach from the trophoblast basement membrane of the villi and aggregate to form columns of unpolarized cells, which attach to the uterine wall. Invasive CTBs, also known as extravillous trophoblasts, deeply invade (interstitially) into the uterine wall, reaching the inner third of the myometrium during normal pregnancy. During

ISSN Print 0013-7227 ISSN Online 1945-7170
Printed in USA

Received 31 August 2016. Accepted 30 January 2017.
First Published Online 8 March 2017

Abbreviations: ANOVA, analysis of variance; AQP, aquaporin; BSA, bovine serum albumin; CK, cytokeratin; CTB, cytotrophoblast; DE, differentially expressed; ECM, extracellular matrix; FC, fold change; FE, fold enrichment; GO, gene ontology; IgG, immunoglobulin G; MMP, matrix metalloproteinase; PBS, phosphate-buffered saline; PE, preeclampsia; qRT-PCR, quantitative reverse transcription polymerase chain reaction; RNA-seq, RNA sequencing; RPKM, reads per kilobase per million mapped reads.

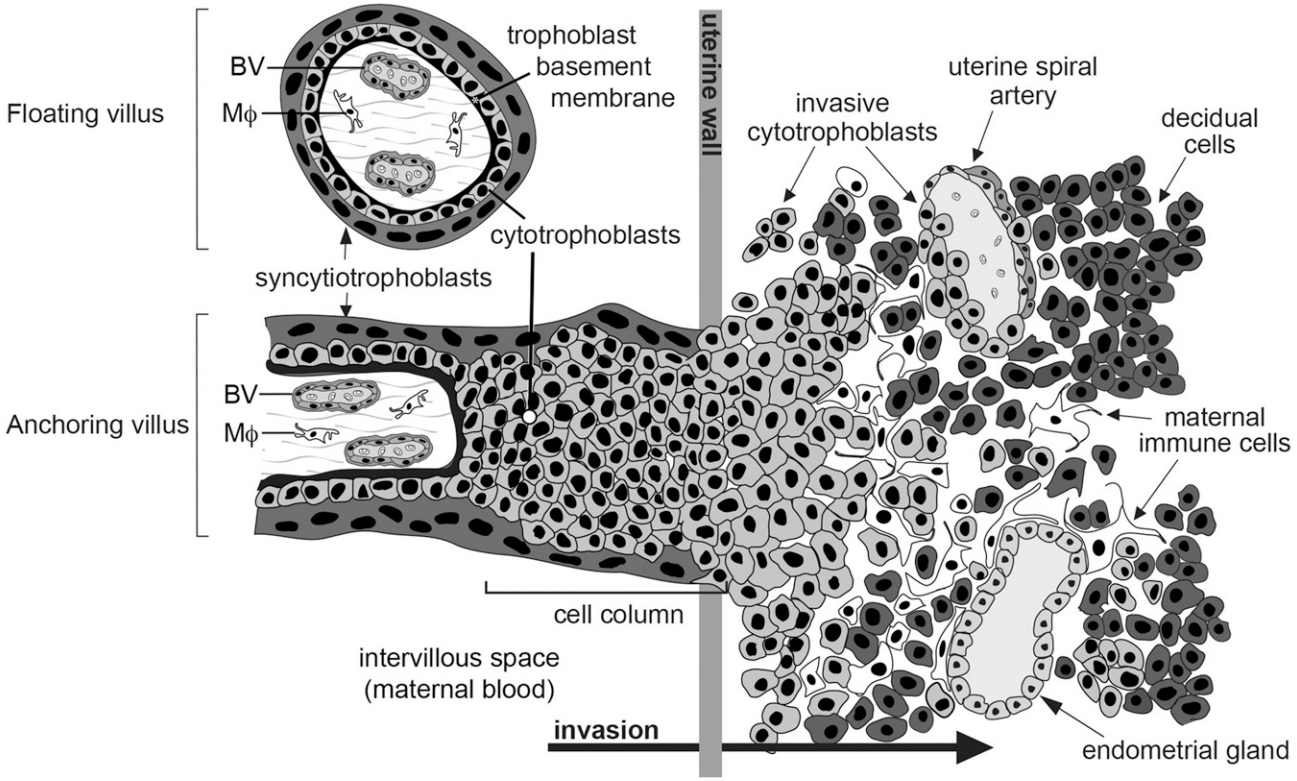

Figure 1. Arrangement of cytotrophoblasts (CTBs) at the human maternal–fetal interface. Within the intervillous space of the human placenta, floating chorionic villi are suspended in circulating maternal blood. These structures facilitate the exchange of nutrients, wastes, and gases between the maternal and embryonic/fetal units. Villi are covered in two trophoblast layers, as follows: (1) an outer layer of multinucleated syncytiotrophoblasts and (2) a polarized layer of mononuclear CTBs. In anchoring chorionic villi during the first and second trimesters of pregnancy, CTBs, which are differentiating along the invasive pathway, exit the placenta by detaching from the trophoblast basement membrane and aggregating to form columns of unpolarized cells, which attach to the uterine wall. CTBs invade the decidua (interstitial invasion) or remodel the uterine spiral arteries (endovascular invasion), which increases their elasticity and diverts maternal blood flow to the placenta. CTB cultures contain cells isolated from floating and anchoring villi. BV, fetal blood vessel; MΦ, macrophage [modified from Damsky *et al.* (1)].

remodeling of the uterine vessels, endovascular CTBs penetrate the walls of the spiral arteries, increasing their diameter, decreasing resistance, and diverting maternal blood flow to the placenta (3, 4). Due to their diverse and important roles in placental development, perturbations in CTB differentiation may be associated with several pregnancy complications, such as preeclampsia (PE) (5) ± intrauterine growth restriction, preterm labor (6), and the syndromes associated with excessive invasion (*e.g.*, accreta, percreta, and increta) (7).

Influenced by numerous cues (8), CTBs modulate the expression of molecules that mediate adhesion, migration, and cell–cell communication, which underlie their broad functional capabilities. For example, as CTBs penetrate the uterine wall, they downregulate the expression of adhesion molecules that inhibit invasion, such as E-cadherin, and upregulate others that favor this process (1). To facilitate invasion, CTBs release numerous degradative molecules, including matrix metalloproteinase (MMP) family members (9), which break down basement membrane components and extracellular matrix (ECM) molecules they encounter. At the same time, the cells upregulate other factors that play a role in their unusual ability to mimic endothelial and vascular smooth muscle cells. These include other adhesion molecules [*e.g.*, VE-cadherin (10), neural cell adhesion molecule (11)] as well as Eph/ephrin and Notch family members (12, 13), which most likely play crucial roles in the ability of endovascular CTBs to channel blood that flows through the maternal spiral arteries, which they line. Furthermore, the cells express a complex network of molecules (*e.g.*, interleukins, chemokines, and HLA-G) that mediate their interactions with the maternal immune system (14). Determining, at a global level, the mechanisms controlling these behaviors (*e.g.*, migration, adhesion, invasion, and immune tolerance), which are critical for CTB functions, is key to understanding normal placental development and disease.

Due to the difficulty of studying human CTBs *in utero* and known differences between human and rodent placentation and pregnancy, primary human cell culture models are valuable because they enable studies that address CTB functions at cellular and molecular levels (15). Over the past 30 years, protocols have been developed for isolating and culturing CTBs from placentas of various gestational ages (16, 17). Multiple steps have been

introduced to improve the viability and purity of CTBs, for example, serial enzymatic digestions, Percoll gradient separations, and magnetic bead immunodepletions (18). In this context, CTBs isolated from normal pregnancies and a variety of pregnancy complications are used to study a wide range of placental cell functions *in vitro*.

Transcriptomic-based approaches provide a means to survey global RNA expression changes at gene and pathway levels. Additionally, the *in vitro* and *in vivo* expression of the identified molecules can be directly compared as an independent measure of their potential relevance to human pregnancy. In placental cells or tissue, global assessments of RNA expression have been used to investigate the molecular changes that occur during pregnancy and the factors that may influence expression, such as gestational age (19), tissue specification (20), species (21), and normal vs disease states (22). This approach has also been used to profile subsets of primary CTBs (23).

Our laboratory routinely isolates and cultures CTBs from first- and second-trimester placentas as well as term tissue. We use this cell culture model to study, at cellular and molecular levels, the differentiation pathway that leads to invasion of the uterine wall (16, 24). In this study, building on this work, we describe CTB morphological transitions and parallel transcriptomic changes over time *in vitro* as the cells acquire an invasive phenotype. The detailed characterization of this culture model during the second trimester of pregnancy will expand the utility of this system for studies of placental development, in normal pregnancy and disease, and for studies of the effects of possible perturbants such as environmental exposures.

Materials and Methods

Tissue collection

All methods in this study were approved by the University of California, San Francisco, Institutional Review Board. Informed consent was obtained from all donors. Second-trimester placentas (gestational age: 14 to 22 weeks) were collected immediately following elective terminations and placed in cytowash medium, consisting of DME/H-21 (Gibco), 12.5% fetal bovine serum (Hyclone), 1% glutamine plus (Atlanta Biologicals), 1% penicillin/streptomycin (Invitrogen), and 0.1% gentamicin (Gibco). Tissue samples were placed on ice prior to dissection.

Human primary villous CTB isolation

CTBs, consisting of both extravillous and villous CTBs, were isolated as described (16), with minor modifications, from second-trimester human placentas (gestational ages ranged from 14 to 22 weeks). In brief, the floating and anchoring chorionic villi were extensively washed in cold phosphate-buffered saline (PBS), dissected into 2- to 4-mm pieces, and filtered through a 1-mm mesh strainer to remove small pieces of tissue. CTBs were isolated according to the following steps: (1) removal of the outer syncytial layer via collagenase (Sigma-Aldrich; C-2674) digestion; (2) release of the CTBs by sequential enzymatic digestion [trypsin (Sigma-Aldrich; T8003; twice) and collagenase]; and (3) purification via Percoll density gradient centrifugation. Single cells were counted using a hemacytometer and immediately collected (0-hour samples) or transferred to a Matrigel (BD Biosciences)-coated 12-well plate. The substrate consisted of a 1:1 (volume-to-volume) mixture of Matrigel and culture medium (see later), which was incubated for 15 minutes at 37°C. CTBs were cultured at a density of 500,000 CTBs/well in 1.5 mL medium containing DME/H-21, 2% Nutridoma (Roche), 1% sodium pyruvate (Sigma-Aldrich), 1% HEPES buffer (Invitrogen), 1% glutamate plus (Atlanta Biologicals), and 1% penicillin/streptomycin (Invitrogen). Cells were incubated at 37°C in 5% CO_2/95% air. At 3 hours postplating, medium was replaced to eliminate unattached cells. As previously reported, staining with anti-cytokeratin (CK) showed that cell purity was routinely ~80% to 90% (16). Only cell preparations that met this criterion were analyzed. Because we analyzed primary CTBs, contaminants (*e.g.*, immune and stromal cells) could contribute to the downstream analyses.

Immunolocalization of CTB antigens

At 3, 15, or 39 hours of culture, medium was removed and cells were washed once with PBS. Next, CTBs were fixed with 4% paraformaldehyde for 20 minutes, washed twice with PBS, and stored in PBS at 4°C until further processing. PBS was removed, and cold methanol was added to permeabilize the CTBs. After 5 minutes, the cells were washed with PBS three times, and 5% bovine serum albumin (BSA) (Hyclone)/PBS was added for 1 hour to block nonspecific reactivity. The blocking solution was removed, the primary antibody (in 5% BSA) was added, and the cells were incubated overnight at 4°C. Primary antibodies included the following: anti-CK [catalogue Fisher_001-clone7D3, Research Resource Identifier (RRID): AB_2631235, rat monoclonal; 1:100] (8), anti-HLA-G (catalogue Fisher_002-clone4H84, RRID:AB_2631236, mouse monoclonal; 1:100) (25), and anti-Ki-67 (Thermo Fisher Scientific catalogue RM-9106-S1, RRID: AB_149792, rabbit monoclonal; 1:100). CKs recognized by the rat antibody are highly expressed by human CTBs vs other placental cell types, possible contaminants (26). HLA-G, a major histocompatibility class Ib antigen, is specific for extravillous CTBs (25, 27). Ki-67 expression, a nuclear antigen, is used to identify proliferating cells (28). The next day, the antibody solution was removed and the CTBs were washed three times in PBS. Detection of primary antibodies was accomplished via incubation (1 hour) with species-specific secondary antibodies diluted in PBS:goat anti-rat immunoglobulin G (IgG; Alexa Fluor, 1:1000, A11081; Life Technologies); donkey anti-mouse (1:1000, A21202; Life Technologies); and goat anti-rabbit IgG (1:1000, A21206; Life Technologies). Cultures were washed with PBS three times and transferred to 1.5 mL PBS mixed with Hoechst 33342 (1:2500; Life Technologies). Phase brightfield and fluorescent photo montages were created by stitching together images (42 covering a 5-mm × 5-mm area), which were captured by using a Leica inverted microscope with a 10× objective and the tilescan function (Leica Application Suite Advanced Fluorescence).

We calculated the average fluorescence intensity associated with CK, HLA-G, or Ki-67 on a per cell basis by using Volocity software (PerkinElmer; version 6.3). First, we identified all cells or objects within each image by virtue of Hoechst staining. Initially, we excluded objects that intersected with the border of the image or were $<20\ \mu m^2$, which eliminated potential artifacts (*e.g.*, cell debris). As a result of this process, ~1% of the

objects were discarded from the analysis. We applied a separation of object function, which included automated erosion and division operations to enable improved measurements of aggregated cell populations. Next, we determined the average intensity of CK, HLA-G, or Ki-67 per object. For CK or HLA-G, we used the dilate function (level 4) to measure the intensity of immunoreactivity associated with the cytoplasm and plasma membrane, respectively. Immunopositive/-negative intensity thresholds for CK or HLA-G immunostaining were determined as the mean intensity of ≥30 objects with negative signal + 1 standard deviation. Thresholds (±) for Ki-67 average intensity were calculated as the mean average intensity of ≥30 objects with immunopositive Ki-67 nuclear signals −1 standard deviation. To control for variability in overall fluorescence intensity among experiments, limits were determined on a per well basis for each experiment and time point. Percentages of cells that expressed each antigen were calculated as the number of immunopositive cells per total number of cells per stitched image. Average values were determined across ≥3 independent cultures. Images captured ~20,000 cellsper well.

Quantification of CTB migration

To describe migration and aggregation of CTBs over time, we determined the minimum distance between nuclei using Volocity software. Objects were identified, as described in the previous section. Then we calculated the minimum distance between nuclei (centroid to centroid). This process entailed automated measurements of all possible distances between objects within each image. Three to 12 stitched images were analyzed per independent experiment (n = 3), and the average minimum distance among cells at 3, 15, and 39 hours postplating was calculated. The standard error of the mean was computed across the average of the three independent experiments. Representative images at 20× were exported in TIF format and processed via Photoshop (Adobe).

RNA isolation

Placentas for transcriptional profiling ranged in gestational age from 14 to 21 weeks (mean = 17.5 weeks). Two experiments used cells from individual placentas, and two experiments used a combination of cells that were isolated from two placentas. The contribution of female and male samples to the data was estimated by evaluating CTB expression (0 hours) of sex-specific genes: RPS4Y1, XIST, EIF1AY, and KDM5D (29) (Supplemental Fig. 1). Information about gestational age and sex is included in Supplemental Table 1. Samples for quantitative reverse transcription polymerase chain reaction (qRT-PCR) validation ranged in gestational age from 18.3 to 22 weeks (mean = 20.3 weeks). RNA for these analyses was isolated from CTBs that were prepared from individual placentas. Briefly, immediately following CTB isolation (0 hours) or after 3, 15, 19, or 39 hours in culture, RLT lysis buffer (Qiagen) was added to either the cell pellet or culture dish well. The lysate was collected and stored at −80°C. We isolated and purified RNA using the RNeasy Micro Kit (Qiagen). The RNA concentration and quality were estimated (absorbance 260 nm/280 nm = 1.9 to 2.1) by using a Nanodrop spectrometer (Thermo Fisher Scientific). Samples destined for microarray analyses (0-, 3-, 15-, and 39-hour time points) were assessed for quality (RNA integrity number > 9) using the Agilent RNA 6000 Nano LabChip Kit and Bioanalyzer 2100 system.

Global gene expression profiling of CTBs

The analysis platform was the Affymetrix Human Genome U133 Plus 2.0 array. Sample processing and hybridization were performed by the University of California, San Francisco, Gladstone Institute, as previously described (29). Affymetrix CEL files were processed using the Affymetrix Expression Console and Transcriptome Analysis Console software packages. Raw values were normalized via the robust multiarray average algorithm. Raw and normalized data were deposited in the Gene Expression Omnibus (GSE86171). One-way analysis of variance (ANOVA) was applied to identify differentially expressed (DE) genes across time. Average fold change (FC) values were determined by calculating the ratio of average log 2 intensities between each time point and the 0-hour CTB group. Datasets were annotated using the Affymetrix Transcriptome Analysis Console database (10/1/14). In cases of multiple probes per gene, the one with the lowest P value, having the most significant change over time, was selected for comparison purposes. To define DE genes across time and among samples, we applied a cutoff of $P \leq 0.00005$ (one-way ANOVA), an absolute FC ≥ 2 between any of the four time points with a false discovery rate of <1%. Hierarchical clustering of FC values was completed by using average linkage and Euclidean distance (TIGR MEV) (30). A secondary *post hoc* Student t test was used to determine the significance of changes between each time point and time 0 hours (cutoff applied: $P \leq 0.001$, absolute FC ≥ 2).

Functional analyses of DE genes

We used DAVID (31) to identify functional enrichment of gene ontology (GO) biological processes (level 4) within our DE gene list. Genes were defined using the Affymetrix Probe ID. GO terms containing ≥15 DE genes with a P value of ≤0.005 and a fold enrichment (FE) ≥1.5 were selected as significantly overrepresented. Corresponding enrichment scores (*i.e.*, P values and FE, were also determined for upregulated and downregulated gene clusters). As previously described (32), relative enrichment scores across GO terms were calculated as $-log\ (p - value) \times FE$. We grouped GO terms based on GO classification (http://geneontology.org) to express common themes. To evaluate changes within GO biological processes on a temporal level, we calculated absolute average FC ratios of DE genes across time within enriched GOs, which were selected based on their relevancy to human placental development.

Validation of DE genes

These analyses used an independent set of CTBs cultured for 0, 3, 15, 19, and 39 hours. First, RNA was converted to complementary DNA using an ISCRIPT complementary DNA synthesis kit (Bio-Rad). Next, qRT-PCR was performed using TaqMan Universal Master Mix II, no UNG (Life Technologies), and specific TaqMan primers for CBS, CXCL6, DHCR7, DUSP2, F5, FABP7, ITGA2, MMP9, MMP12, PDXK, PEG3, and S100A7 (Supplemental Table 2). Selected targets were identified based on observations of robust (absolute FC > 2) and significant ($P < 0.0005$) changes in expression over time, and association with pathways of interest. We also included PEG3 ($P = 0.005$, absolute FC > 2) and MMP12 ($P = 0.4$) to estimate the repeatability of targets with different significance criteria. Reactions were carried out for 40 cycles. A minimum of three biological replicates was analyzed in all comparisons. Differential expression across time was calculated by using the ΔΔ cycle threshold method (normalized

to glyceraldehyde-3-phosphate dehydrogenase). To determine significant changes over time, one-way ANOVA was applied ($P \leq 0.05$). FC values were expressed as average log 2 ratios between each time point and the 0-hour CTB group.

Comparisons between second-trimester and term samples

We assessed the expression profiles of genes identified to be DE in CTB culture in an RNA sequencing (RNA-seq) dataset generated by the Epigenome Roadmap Project (20), which included CTBs purified, in our laboratory, from second-trimester and term placentas (0 hours). We compared the average reads per kilobase per million mapped reads (RPKM) expression values of second-trimester and term CTBs with differences in expression between these time periods. The official gene symbol was used to align the two datasets (merge function) (33).

Immunostaining of tissue sections

We used an immunolocalization approach to investigate the expression, at the protein level, of transcripts that were abundant as well as DE over time in cultured CTBs. For this purpose, we analyzed tissue sections of the maternal–fetal interface during the second trimester of pregnancy. The general method we used was published (34). Briefly, biopsies were fixed in 3% paraformaldehyde, dehydrated in increasing sucrose concentrations, and embedded in OCT (Thermo Fisher Scientific). Immunolocalization of proteins was performed using species-specific primary antibodies diluted in blocking buffer (PBS with 3% BSA and 0.05% Tween 20) for anti-CK (rat polyclonal; 1:100) (8), anti-NOTUM (Sigma-Aldrich; catalogue SAB3500082, RRID: AB_10604118, rabbit polyclonal, 1:100), and anti-EFEMP1 (Abcam; catalogue ab14926, RRID:AB_301517, rabbit polyclonal, 1:100) for 1 hour at 37°C. Detection of primary antibodies was done via incubation (1 hour at 37°C) with species-specific secondary antibodies diluted in blocking buffer: goat anti-rat IgG (Alexa Fluor, 1:1000, A11081; Life Technologies) and goat anti-rabbit IgG (1:1000, A21206; Life Technologies). Sections were washed with PBS three times and coverslipped with Vectashield containing 4′6-diamidino-2-phenylindole (Vector Bio-Laboratories). For these analyses, tissue sections from at least 12 placentas were evaluated. Images were acquired using a Leica inverted microscope with a 10× or 20× objective. Representative photomicrographs were exported in TIF format and processed via Photoshop (Adobe). No specific immunoreactivity was detected staining with the primary or secondary antibody alone or with an irrelevant isotype-matched antibody.

Results

Characterization of cultured CTBs

CTBs, isolated from floating and anchoring chorionic villi of second-trimester placentas, were plated on Matrigel and cultured for up to 39 hours. Within 3 hours, CTBs started to spread on the matrix and extend cellular projections [Fig. 2(a–c)]. By 15 hours, CTBs formed multicellular aggregates. Time-lapse imaging indicated a high level of cell movement within the aggregates at higher resolution (data not shown). Furthermore, as previously described (16), CTBs did not fuse to form multinucleated syncytiotrophoblasts. To complement our visual observations, we quantified the distance of each CTB to its closest neighbor at 3, 15, and 39 hours. We observed a significant difference in the average minimum distance among cells at 15 hours ($\Delta\downarrow 4.5$ μm) as compared with 3 hours [$P \leq 0.05$; Fig. 2(d)]. Cell aggregation was similar at 15 and 39 hours ($P \geq 0.05$). Using a semiquantitative approach that combined immunofluorescence localization and high-throughput content image analysis, we calculated (on average) that the majority of cells in our model expressed CK (86.1 ± 1.6%) [Fig. 2(e)] and HLA-G (72.3 ± 4.4%) [Fig. 2(f)]. In contrast, only 2.1 ± 0.6% of cells expressed Ki-67 [Fig. 2(g)]. The expression of CK, HLA-G, and Ki-67 did not change as a function of time in culture [quantified in Fig. 2(h)]. As a whole, these observations suggested that our tissue culture system models CTB exit from the cell cycle aggregation, a proxy for differentiation.

We identified 2232 genes as significantly DE across time (0–39 hours) as CTBs differentiated in culture (ANOVA, $P \leq 0.00005$, absolute FC ≥ 2) [Fig. 3(a)]. Within this gene set, time-dependent changes were highly dynamic. Approximately 54% of DE genes followed a positive trend across time (Cluster I), and conversely, 46% of DE genes displayed a negative trend (Cluster II). As compared with the 0-hour data, the largest differences, in terms of absolute magnitude and significance, were observed at 15 hours [Fig. 3(b)]. These analyses suggested robust time-dependent changes in the transcriptome of CTBs during the initial 39 hours of culture.

As to the DE subset, we observed an enrichment of genes involved in a diverse range of GO biological processes, including anatomical structural morphogenesis, vasculature development, cell motion, RNA metabolism, translation, monosaccharide metabolism, energy derivation by oxidation of organic compounds, inflammatory response, coenzyme metabolism, regulation of cell proliferation, and apoptosis ($P \leq 0.005$, FE ≥ 1.5) [Fig. 4(a)]. We also conducted separate GO analyses for Clusters I or II. On average, genes that were involved in RNA metabolism and energy derivation were upregulated over time. This was particularly true for RNAs encoding proteins that function in the electron transport chain (30↑, 2↓). Enriched categories of genes that were predominately downregulated over time in culture included response to lipopolysaccharide (6↑, 15↓) and regulation of proliferation (20↑, 47↓).

With regard to selected GO categories, expression of genes related to inflammatory responses, anatomical structure morphogenesis, regulation of cell migration/motion, apoptosis, RNA metabolism, and electron transport chain changed in a time-dependent manner, peaking at 15 hours [absolute FC; Fig. 4(b)]. For example, at this time point there was a fourfold change in expression of genes that are

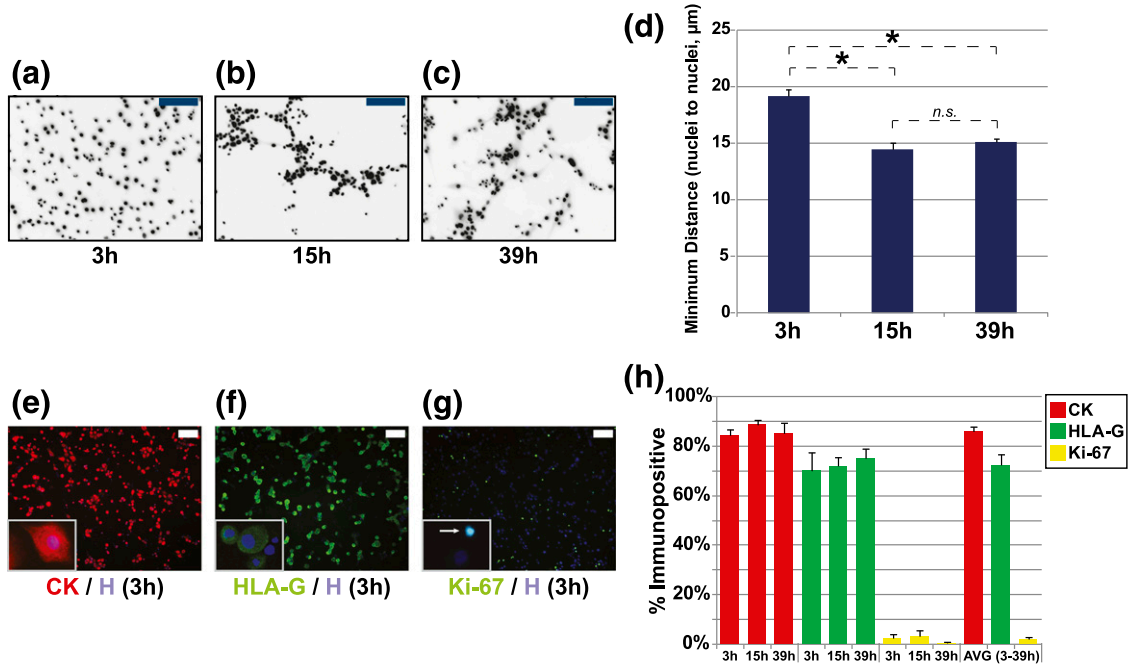

Figure 2. Morphological transitions of cultured primary human CTBs over 39 hours. (a–c) CTBs were incubated for 3, 15, and 39 hours before the nuclei were visualized by Hoechst staining. (d) The average minimum distance among CTB nuclei (n = 3). Asterisks signify $P \leq 0.05$ (*t* test). Representative images of immunostaining for (e) CK, (f) HLA-G, and (g) Ki-67 in CTBs at 3 hours; nuclei were stained with Hoechst. (h) Average percentage of cells that stained for these antigens as a function of time in culture. Images are representative of ≥3 independent experiments. Scale bars = 100 µm. n.s., not significant.

involved in inflammatory responses (log 2 = 2.0). In contrast, the expression of genes related to vitamin responses and vascular development peaked at 39 hours with the highest observed FCs, 6.4 (log 2 = 2.7) and 3.3 (log 2 = 1.7), respectively.

Due to our interest in the mechanisms underlying CTB differentiation/invasion and vascular mimicry, we mapped DE genes (additional filter; absolute FC > 4) associated with three GO biological processes: anatomical structure morphogenesis (28 genes), cell motion (the family term of cell migration; 18 genes), and vasculature development (23 genes) [Fig. 5(a)]. This gene subset included ITGA2, S100A7, ETS1, EDN1, IL6, DHCR7, MMP9, and CD44, which were upregulated over time, and DLX6, FOXC1, KISS1R, DLX5, FLT1, BMP7, NR4A3, and CITED2, which were downregulated. Molecules linked to response to vitamin were also clustered due to their strong regulation and the influence of vitamins on pregnancy outcome. This subset included p450 enzymes (CYP1A1, -27B1), the vitamin D receptor, CD44, and aquaporin (AQP)3, which were all upregulated in culture [Fig. 5(b)]. We also listed DE genes with the largest FCs in our culture system. This subset included a variety of molecules that are linked to the aforementioned categories and additional pathways, including chemokines and inflammatory molecules (*e.g.*, CFB, SAA1, TNFAIP6, CXCL5, and CXCL6), collagen endopeptidases (MMP3, -10), solute carriers (SCL22A1, -6A11, -1A6), and structural components (*e.g.*, KRT6A, KRT6B, ITGA2, and LAMB3) (Supplemental Table 3).

For a subset of DE genes, we validated expression changes observed by microarray via a qRT-PCR approach and RNA samples isolated from a second set of CTB samples [Fig. 5(c)]. DHCR7, PDXK, CD44, CBS, MMP9, CXCL6, ITGA2, and S100A7 were upregulated with time

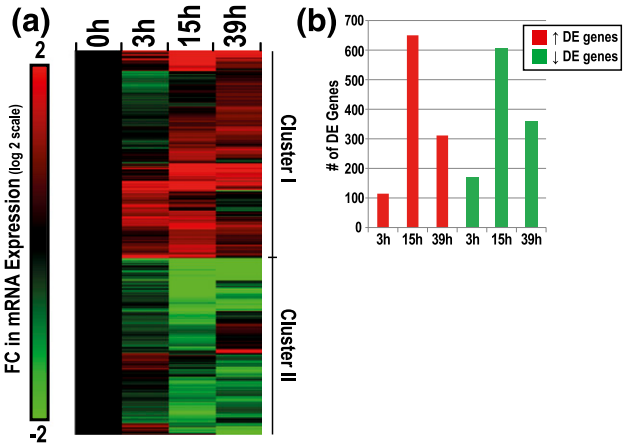

Figure 3. Characterization of changes in CTB gene expression as a function of time in culture. (a) Hierarchical clustering of time-dependent DE genes in CTBs (2232 genes total, $P \leq 0.00005$, absolute FC ≥ 2). Upregulated or downregulated genes over time in culture were designated as either cluster I or cluster II, respectively. Average FC values are displayed as the ratio of average intensities between each time point and the average 0-hour CTB values (log 2 scale). (b) *Post hoc t* test analysis of DE genes per time point (*t* test, $P \leq 0.001$, absolute FC ≥ 2).

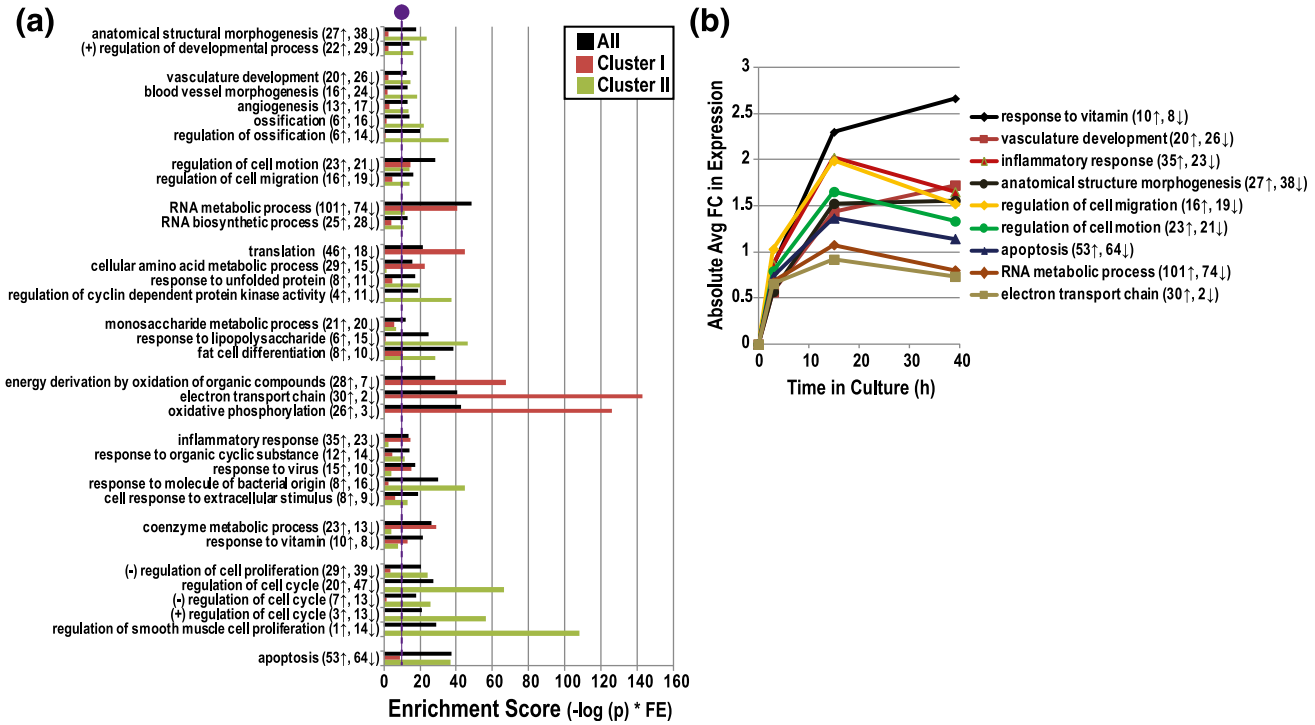

Figure 4. Functional GO enrichment analysis of CTB genes that were upregulated or downregulated as a function of time in culture. (a) GO terms that were overrepresented (biological processes) among DE genes whose expression changed during CTB culture ($P \leq 0.005$; FE ≥ 1.5, total number changed ≥ 15; bar denotes significance). (b) Absolute average FC ratios of DE genes within selected enriched GO terms. The number of upregulated or downregulated DE genes in each category. (+), positive; (−), negative.

in culture (ANOVA, $P < 0.05$). F5, DUSP2, FABP7, and PEG3 were downregulated (ANOVA, $P < 0.05$). MMP12 mRNA levels, which did not change according to the microarray data, were also unchanged when assayed by qRT-PCR. Our qRT-PCR and microarray results were highly correlated in terms of FC in expression (as compared with the 0-hour time point) ($r = 0.88$; not shown). FC values for genes (PDXK, PEG3), which were not significantly regulated in the microarray data ($0.05 > x > 0.0005$), correlated between the two analytical methods.

We tested the hypothesis that gene expression changes *in vitro* parallel, in some cases, genes and pathways that are upregulated in second trimester, when the placenta is still remodeling the uterine wall, as compared with term, when this process is completed. Thus, we interrogated ssRNA-seq profiles of freshly isolated CTBs from second-trimester and term placentas (20) to determine transcripts (identified as DE *in vitro*) whose expression was dependent on gestational age. Of the 2232 DE genes *in vitro*, 1955 had RPKM values [Fig. 6(a)]. We plotted the average abundance of this subset vs the FC difference in expression between second-trimester and term CTBs [Fig. 6(b)]. Approximately 95% of the genes we compared were expressed >1 RPKM (log 2 scale = 0). Approximately 16% of genes were DE >twofold between the two gestational ages (blue lines, log 2 scale = 1). Forty-seven genes that were in the 10th percentile by abundance (>58.5 RPKM) were also gestationally regulated (>twofold). This subset included molecules upregulated in term vs second-trimester CTBs (*e.g.*, EFEMP1) or upregulated in second-trimester vs term CTBs (*e.g.*, NOTUM). The majority of genes that were modulated during gestation (77%) were downregulated (green vs red) in culture. Furthermore, we conducted additional analyses using the subset of genes (105 total) that was associated with pathways underlying CTB differentiation/invasion: anatomical structure morphogenesis, cell motion, and vasculature development [Fig. 6(c)]. This subset included molecules upregulated in term vs second-trimester CTBs (*e.g.*, BMP7, KLF4, and JAG1) or upregulated in second-trimester vs term CTBs (*e.g.*, MMP9, ITGB3, and IL6R). Thus, the latter cross comparison identified molecules that are known regulators of CTB invasion, suggesting that potentially novel candidates that emerged from this analysis could be interesting to study in this context.

Next, in tissue sections of second-trimester biopsies of the maternal–fetal interface, we evaluated protein expression of NOTUM and EFEMP1 using an immunofluorescence approach. These two molecules stood out in our transcriptomic analyses as follows: (1) highly abundant; (2) significantly DE over time in cultured CTBs; and (3) DE between second trimester and term. In second-trimester tissue sections (n = 12), NOTUM [green; Fig. 7(a)] was expressed in all trophoblast subpopulations that we

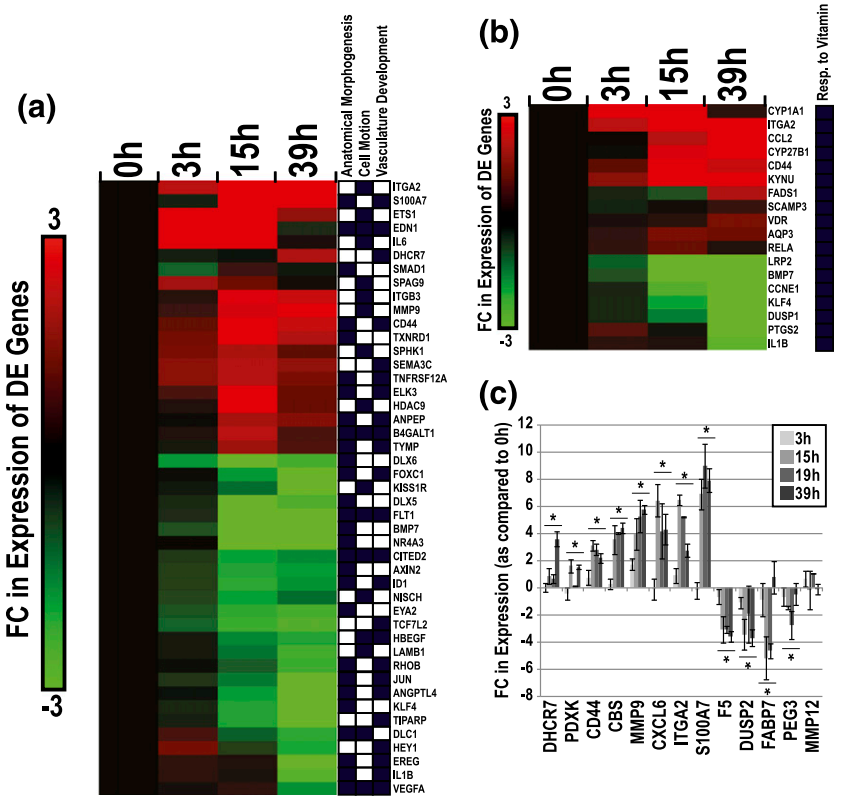

Figure 5. DE genes within enriched categories relevant to CTB invasion. (a) Hierarchical clustering plot of DE genes related to enriched GO terms (anatomical structure morphogenesis, cell motion, and vascular development) in CTBs over time in culture. DE genes that passed a secondary filter (absolute FC > 4; log 2 = 2) are shown. Black boxes signify GO associations. (b) DE genes related to the enriched GO term: response to vitamin. (c) qRT-PCR verification of gene expression changes over time in culture. Asterisks indicate significant changes (ANOVA, $P \leq 0.05$; bars denote standard error of the mean).

examined, including CTBs within the floating villi and cell columns (upper panels) as well as the placental cells that invaded more deeply into the decidua (lower panels). Expression of NOTUM was also apparent in non-CK–positive cells within the villous core and decidua. As to modulation as a function of invasion, the major finding was that NOTUM expression tended to move from the cytoplasm to the nucleus. EFEMP1 was also widely expressed among the CTB subpopulations [Fig. 7(b)]. In general, antibody reactivity, which was highest in villous CTBs (upper panels), decreased as the cells invaded the uterus (lower panels). Thus, these analyses suggested that NOTUM and EFEMP1 have interesting patterns of modulation as a function of CTB differentiation/invasion.

Discussion

Model systems in which TBs isolated from human placentas are placed in culture provide important opportunities for studying the mechanisms and cellular functions underlying normal development and disease. We published protocols for isolating CTBs and culturing them on three-dimensional substrates (16, 24). Targeted analyses showed that under these conditions the cells differentiate along the pathway that leads to migration away from the placenta proper and invasion of the uterine wall (1, 8). In this work, we expanded these reports by completing a global transcriptomic analysis that described in detail the changes in gene expression that paralleled the CTB morphological transitions as the cells acquired an invasive phenotype *in vitro*. Later we discuss these results in the context of CTB differentiation *in vivo*.

Quantification of CTB migration *in vitro*

We developed a semiautomated pipeline for doing high throughput image content analysis and applied this approach to our CTB differentiation model. As described previously, the majority of cells expressed CK, which identifies all TB subpopulations, and HLA-G, which is upregulated at the protein level as the cells invade the uterine wall (25, 26). Isolation and culture of second-trimester CTBs on Matrigel enabled their attachment (by 3 hours), after which they spread on the substrate, becoming highly migratory. In the process, they migrated toward each other, forming multicellular aggregates while extending elongated filapodia (by 15 hours). In agreement with previous studies, we showed that cultured CTBs that differentiated along the invasive pathway had a very low rate of proliferation (~2% immunopositive for Ki-67 expression). We quantified these transitions by measuring the average minimum distance between the cell nuclei at three time points. This approach enabled us to quantify migratory activity and aggregation across hundreds of thousands of cells. In this study, we established baseline conditions that, in future experiments, can be used to evaluate the effects of potential perturbants, including pharmaceuticals, environmental chemicals, and disease states (35), on CTB behavior.

Transcriptomic changes in cultured CTBs

In parallel with the described morphological transitions, we observed robust, global RNA expression changes over time in cultured CTBs (Fig. 3). Using a conservative approach (false discovery rate <1%; $P \leq 0.00005$; absolute FC ≥2), ~10% of genes were significantly DE over time. Our results suggested changes in

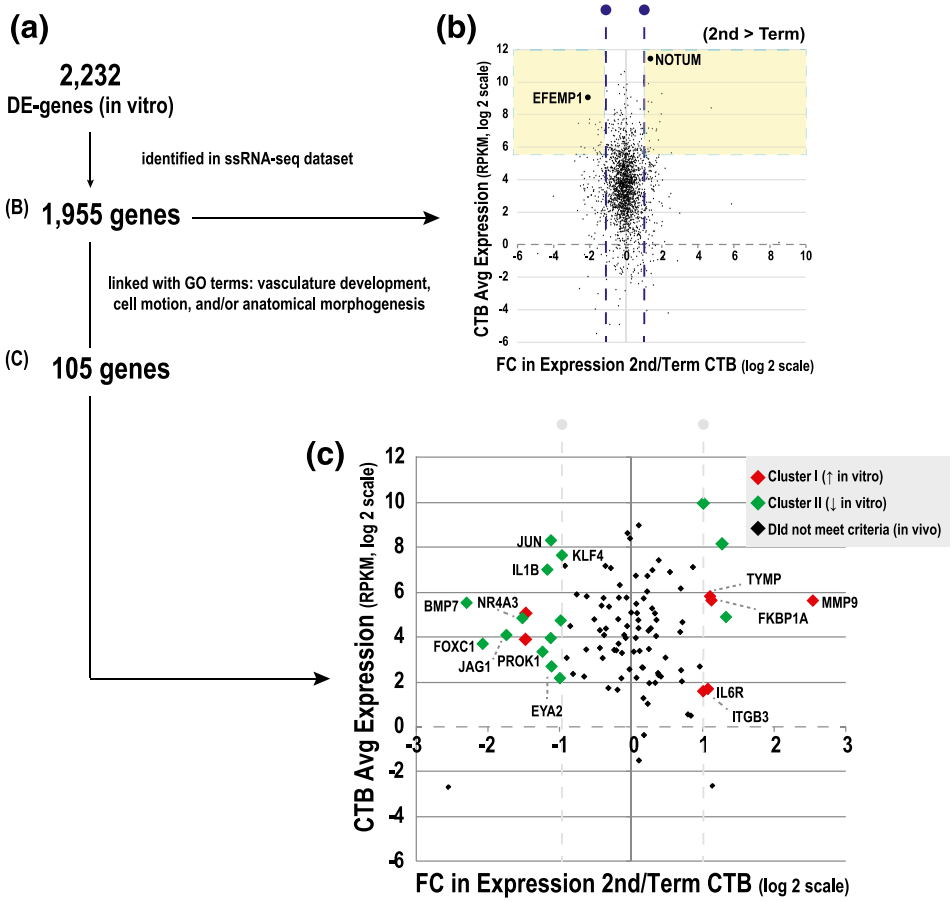

Figure 6. Mapping CTB genes that were DE in culture (microarray) to CTB gene expression changes from second trimester to term (RNA-seq). (a) The RNA-seq dataset was generated from CTBs that were isolated in our laboratory (20). In total, 1955/2232 DE genes could be compared. (b) The average abundance of transcripts of DE genes (*y*-axis, RPKM, log 2 scale) vs the FC difference between second-trimester and term CTBs (*x*-axis, log 2 scale). (c) DE genes related to GO terms: anatomical morphogenesis, cell motion, and/or vascular development. Genes are labeled based on patterns of regulation over time in culture.

specific pathways related to CTB functions *in vivo*, including morphogenesis, vasculature development, cell migration, cell communication, vitamin/nutrition, and inflammatory responses. These pathways suggested an interplay between molecules that drive cell behaviors in CTBs (remodeling, migration), placental development, and cell–cell communication. The data highlighted many interesting processes with known or potential relevance to CTB interactions with maternal cells *in vivo* and novel regulators.

Migration and morphogenesis pathways

At a transcriptomic level, several of the DE molecules played critical roles in CTB migration and/or morphogenesis [Figs. 4 and 5(a)]. This subset included MMP9, which was upregulated (>ninefold) in culture. In parallel, we observed the increased expression of four other MMP family members (MMP3, -8, -10, and -14). As a class, MMPs are critical for CTB invasion and differentiation with MMP9 playing an especially important role (*in vitro* and *in vivo*) (36–38). Lower expression levels of MMP9 are associated with PE (39), and the MMP9 (–1562C/T) variant is linked with PE susceptibility (40). Integrin expression was also modulated, including ITGA2 (↑), ITGB3 (↑) (Fig. 5), ITGB6 (↑), and ITGB5 (↓) (data not shown). Regulated expression of integrins and their ECM ligands is an integral part of the CTB differentiation pathway that leads to formation of cell columns and uterine invasion (41, 42). For example, in first-trimester placentas, column CTBs express high levels of ITGA6/B4 and low levels of ITGA5/B1, whereas invasive extravillous CTBs have the opposite expression pattern (43). To our knowledge, expression of ITGA2 has yet to be described in human CTBs. We identified many other genes that were DE in culture with proposed links to CTB invasion/differentiation and placental development. They included the following: (1) ETS1 (↑), a transcription factor that regulates expression of MMPs and other molecules important for uterine invasion (44, 45); (2) the secreted preproprotein/signaling peptide, EDN1 (↑), which is involved in invasion and vasoconstriction (46); and (3) KISS1R1 (↓), a G protein–coupled receptor that

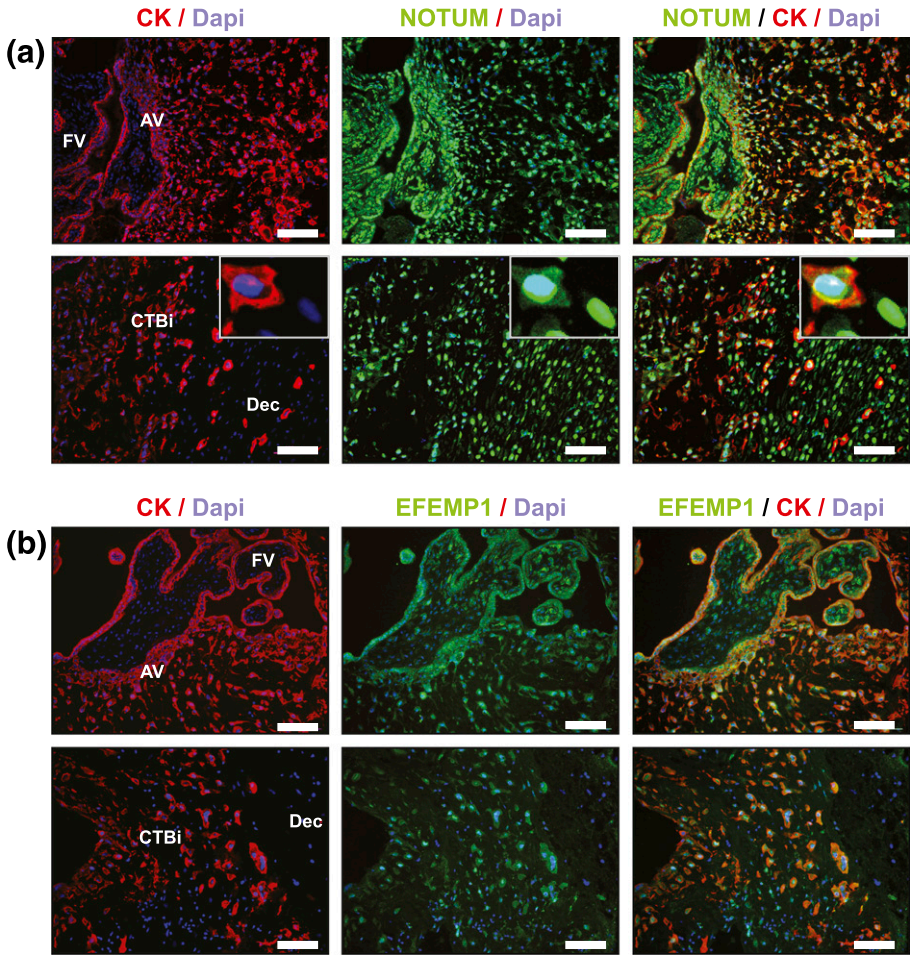

Figure 7. Immunolocalization of NOTUM and EFEMP1, which were DE in cultured CTBs. Representative images of floating and anchoring villi (FV, AV, respectively; upper panels) and invasive (i) CTBs within the decidua (Dec; lower panels). Tissue sections of second-trimester samples were immunostained for (a) NOTUM or (b) EFEMP1. The samples were costained with anti-CK (trophoblast marker) and 4′6-diamidino-2-phenylindole (Dapi; nuclear dye). Tissue sections from ≥12 placentas were evaluated. Scale bars = 100 μm.

selectively binds to kisspeptins and represses TB migration/invasion (47). Our results suggested that CTB differentiation *in vitro* recapitulated many of the molecular switches that occur as CTBs acquire invasive/migratory properties *in vivo*.

Vascular and immune pathways

CTB endovascular invasion garners a supply of maternal blood that enables exchange of nutrients, wastes, and gases at the maternal–fetal interface. In our culture model, DE genes included molecules that play important roles in vascular development [Fig. 5(a)], such as CD44 (↑), a cell adhesion surface receptor for hyaluronic acid and a major component of the ECM. These receptor–ligand complexes regulate intracellular signaling pathways critical for CTB invasion and remodeling of the decidua (48). Other DE molecules in this class included VEGFA and FLT1, which were downregulated. Increased expression of these molecules underlies maternal vascular dysfunction in PE (49). Additionally, several inflammatory mediators were DE in our model. For example, CXCL6 [Fig. 5(c)] and interleukin-6 [Fig. 5(a)] were upregulated. In HTR-8/SVneo cells, interleukin-6 promotes migration, invasion, and modulation of integrin profiles (50). In the same cell line (and in primary CTBs), CXCL6 reduces TB migration/invasion by reducing MMP2 activity (51). Other DE inflammatory molecules included numerous chemokines and interleukins. These results provided a global transcriptional context for previous (13) and future investigations using this model system to study inflammatory mediators and their mechanistic roles in CTB differentiation/invasion, vascular remodeling, and immune interactions with the mother.

Vitamin and nutrient regulation pathways in CTBs

In general, the importance of vitamins and other nutrients for pregnancy health and placental development is well-recognized (52–54). However, the underlying mechanistic links remain unresolved at molecular and cellular levels. In cultured CTBs, genes associated with the GO

term, response to vitamin, were among some of the most dramatically differentially expressed in our dataset [Fig. 5(b)]. This subset included members of the vitamin D signaling pathway—the primary p450-activating enzyme (CYP27B1) and the vitamin D receptor. The expression of both increased with time in culture, suggesting enhanced CTB responsiveness to compounds of this class as they differentiate along the invasive pathway. This observation is in line with published results regarding the relationships between vitamin D and the following: (1) extravillous TB invasiveness (55); (2) calciotropic hormone regulation (56); and (3) pregnancy complications [*e.g.*, PE (57)]. In addition, we observed increased expression of CBS, a member of the folate metabolism/cysteine-synthesis pathway [Fig. 5(c)]. CBS is the critical regulator of homocysteine production during pregnancy, and altered levels may underlie impaired decidualization/changes in uterine–gene expression (58), PE, pregnancy loss, and congenital birth defects (54). The cytochrome p450 enzymes—CYP1A1, -1A2, -1B1—which play roles in xenobiotic/drug metabolism as well as endogenous regulation of fatty acid metabolism, angiogenesis, and epithelial differentiation (59), were also upregulated in culture. The functions of these enzymes, with dual roles in metabolizing exogenous and endogenous compounds, are poorly understood in the context of placental development and function. Additionally, other molecules in this subset, such as AQP3 and AQP9, were upregulated in culture. These membrane proteins, which act as access points for water molecules, may play key roles during mammalian pregnancy (60, 61). Whether these molecules, which are highly regulated in our system, also play roles in CTB differentiation is an interesting possibility.

DE genes in second-trimester vs term CTBs

Using an ssRNA-seq dataset generated as part of the Epigenome Roadmap Project (20), we defined a subset of genes (initially observed to be DE *in vitro* in CTBs) that were DE between second trimester vs term [Fig. 6(a)]. This analysis revealed several abundant molecules (top 10% expression, yellow shading) that were associated with faulty CTB invasion and/or placental disease, *e.g.*, FSTL3 (62), FLT1 (63), ADAM12 (64), TFPI2 (65, 66), F5 (67), and HSD17B1 (68) (Supplemental Table 4), as well as new molecules yet to be studied in this context (*e.g.*, EFEMP1 and NOTUM) [Fig. 6(b)]. In a follow-up analysis, we identified genes that were up- or down-regulated as a function of CTB differentiation/invasion *in vitro*, focusing on a subset of the component processes—morphogenesis, cell motion, and vascular development. Then we asked whether they were also regulated as a function of gestational age [Fig. 6(c)]. Molecules with known functions during CTB differentiation, such as MMP9 (36–38) and ITGB3 (69), were upregulated in cultured CTBs, and the transcripts were expressed at higher levels during second trimester relative to term. In general, these findings further supported the concept that genes and pathways critical to CTB differentiation and placental development were actively modulated in our cell culture model. Furthermore, these analyses highlighted new molecules yet to be studied in this context. For example, we identified two genes, NOTUM and EFEMP1, as potentially involved in CTB differentiation. *In vitro*, aggregating CTBs downregulated their expression at the RNA level. Immunolocalization of NOTUM and EFEMP1, in tissue sections of second-trimester placentas, confirmed expression of these molecules at the protein level in villous CTB progenitors, as well as in CTBs transiting through the columns and within the uterine wall. NOTUM, a carboxylesterase, was recently identified as a key inhibitor of WNT signaling (70) and critical for neural/head induction in *Xenopus* (71). Despite the recognized importance of WNT signaling in TB invasion (72), nothing is known about the potential role(s) of NOTUM in placental development. In our analyses, CTB invasion was associated with movement of NOTUM from the cytoplasmic to the nuclear compartment. To our knowledge, this phenomenon has not been previously reported.

The ECM glycoprotein, EFEMP1, acts as a regulator of MMP expression and cancer metastasis (73). In an estrogen-dependent manner, EFEMP1 inhibits WNT/B-catenin signaling pathways and thereby the epithelial-to-mesenchymal transition of endometrial carcinoma cells (74). Previously, EFEMP1 was shown to be expressed in human CTBs that reside within the smooth chorion layer of fetal membranes (75). In this study, we add new data, suggesting expression of EFEMP1 in the placenta during midgestation and differential patterning of EFEMP1 in villous CTBs (higher expression) as compared with CTBs invading the uterus (lower expression). In general, our study provides evidence of modulation of NOTUM and EFEMP1 expression in CTBs within the maternal–fetal interface, suggesting possible roles of these two molecules in TB differentiation.

Conclusion

Primary cultures of human villous CTBs are an important model system for studying their adhesion, migration, and invasion—behaviors that are critical determinants of pregnancy outcomes. In this study, using a transcriptomic-based approach, we profiled CTB gene expression as the cells differentiated along the invasive pathway *in vitro*. The DE genes were involved in key biological pathways that are critical to placentation *in vivo*: cell migration, vascular remodeling, morphogenesis, and

Appendix: Primary Antibodies

Peptide/ Protein Target	RRID	Antigen Sequence (if Known)	Name of Antibody	Manufacturer, Catalog No., and/or Name of Individual Providing the Antibody	Species Raised in; Monoclonal or Polyclonal	Dilution Used
Cytokeratin	AB_2631235		Clone 7D3	Fisher_001-clone7D3	Rat; monoclonal	1:100
HLA-G	AB_2631236		Clone 4H84	Fisher_002-clone4H84	Mouse; monoclonal	1:100
Ki-67	AB_149792		Ki-67	Thermo Fisher Scientific, RM-9106-S1	Rabbit; monoclonal	1:100
NOTUM	AB_10604118		NOTUM	Sigma-Aldrich, SAB3500082	Rabbit; polyclonal	1:100
EFEMP1	AB_301517	TYTQCTDGYEWDPVRQQC	EFEMP1	Abcam, ab14926	Rabbit; polyclonal	1:100

Abbreviation: RRID, Research Resource Identifier.

inflammation. The rich datasets that were generated provide a foundation of gene expression profiles against which the effects of numerous variables, including environmental and pharmacological compounds, can be evaluated.

Acknowledgments

We thank Cheryl Godwin de Medina for patient recruitment, Gabriel Goldfien and Yan Zhou for technical assistance, and Jason Farrell and Nicomedes Abello for tissue collection.

Address all correspondence and requests for reprints to: Joshua F. Robinson, PhD, Center for Reproductive Sciences, Department of Obstetrics, Gynecology, and Reproductive Sciences, University of California, San Francisco, Box 0665, Room RMB-902E, 35 Medical Center Way, San Francisco, California 94143-0665. E-mail: Joshua.Robinson@ucsf.edu.

This work was supported by the National Institute of Environmental Health Sciences (Grants P01ES022841 and K99ES023846) and the Environmental Protection Agency (Grant RD83543301).

Disclosure Summary: The authors have nothing to disclose.

References

1. Damsky CH, Fitzgerald ML, Fisher SJ. Distribution patterns of extracellular matrix components and adhesion receptors are intricately modulated during first trimester cytotrophoblast differentiation along the invasive pathway, in vivo. *J Clin Invest*. 1992;**89**(1):210–222.
2. Red-Horse K, Zhou Y, Genbacev O, Prakobphol A, Foulk R, McMaster M, Fisher SJ. Trophoblast differentiation during embryo implantation and formation of the maternal-fetal interface. *J Clin Invest*. 2004;**114**(6):744–754.
3. Zhou Y, Fisher SJ, Janatpour M, Genbacev O, Dejana E, Wheelock M, Damsky CH. Human cytotrophoblasts adopt a vascular phenotype as they differentiate: a strategy for successful endovascular invasion? *J Clin Invest*. 1997;**99**(9):2139–2151.
4. Zhou Y, Damsky CH, Fisher SJ. Preeclampsia is associated with failure of human cytotrophoblasts to mimic a vascular adhesion phenotype: one cause of defective endovascular invasion in this syndrome? *J Clin Invest*. 1997;**99**(9):2152–2164.
5. Ball E, Bulmer JN, Ayis S, Lyall F, Robson SC. Late sporadic miscarriage is associated with abnormalities in spiral artery transformation and trophoblast invasion. *J Pathol*. 2006;**208**(4):535–542.
6. Romero R, Dey SK, Fisher SJ. Preterm labor: one syndrome, many causes. *Science*. 2014;**345**(6198):760–765.
7. Jauniaux E, Jurkovic D. Placenta accreta: pathogenesis of a 20th century iatrogenic uterine disease. *Placenta*. 2012;**33**(4):244–251.
8. Chen JZ, Sheehan PM, Brennecke SP, Keogh RJ. Vessel remodelling, pregnancy hormones and extravillous trophoblast function. *Mol Cell Endocrinol*. 2012;**349**(2):138–144.
9. Cohen M, Bischof P. Factors regulating trophoblast invasion. *Gynecol Obstet Invest*. 2007;**64**(3):126–130.
10. Kokkinos MI, Murthi P, Wafai R, Thompson EW, Newgreen DF. Cadherins in the human placenta–epithelial-mesenchymal transition (EMT) and placental development. *Placenta*. 2010;**31**(9):747–755.
11. Blankenship TN, King BF. Macaque intra-arterial trophoblast and extravillous trophoblast of the cell columns and cytotrophoblastic shell express neural cell adhesion molecule (NCAM). *Anat Rec*. 1996;**245**(3):525–531.
12. Hunkapiller NM, Gasperowicz M, Kapidzic M, Plaks V, Maltepe E, Kitajewski J, Cross JC, Fisher SJ. A role for Notch signaling in trophoblast endovascular invasion and in the pathogenesis of preeclampsia. *Development*. 2011;**138**(14):2987–2998.
13. Red-Horse K, Kapidzic M, Zhou Y, Feng KT, Singh H, Fisher SJ. EPHB4 regulates chemokine-evoked trophoblast responses: a mechanism for incorporating the human placenta into the maternal circulation. *Development*. 2005;**132**(18):4097–4106.
14. Hemberger M. Immune balance at the foeto-maternal interface as the fulcrum of reproductive success. *J Reprod Immunol*. 2013;**97**(1):36–42.
15. Orendi K, Kivity V, Sammar M, Grimpel Y, Gonen R, Meiri H, Lubzens E, Huppertz B. Placental and trophoblastic in vitro models to study preventive and therapeutic agents for preeclampsia. *Placenta*. 2011;**32**(Suppl):S49–S54.
16. Hunkapiller NM, Fisher SJ. Chapter 12. Placental remodeling of the uterine vasculature. *Methods Enzymol*. 2008;**445**:281–302.
17. Kliman HJ, Nestler JE, Sermasi E, Sanger JM, Strauss JF III. Purification, characterization, and in vitro differentiation of cytotrophoblasts from human term placentae. *Endocrinology*. 1986;**118**(4):1567–1582.
18. Douglas GC, King BF. Isolation of pure villous cytotrophoblast from term human placenta using immunomagnetic microspheres. *J Immunol Methods*. 1989;**119**(2):259–268.
19. Mikheev AM, Nabekura T, Kaddoumi A, Bammler TK, Govindarajan R, Hebert MF, Unadkat JD. Profiling gene expression in human placentae of different gestational ages: an OPRU Network and UW SCOR Study. *Reprod Sci*. 2008;**15**(9):866–877.
20. Kundaje A, Meuleman W, Ernst J, Bilenky M, Yen A, Heravi-Moussavi A, Kheradpour P, Zhang Z, Wang J, Ziller MJ, Amin V, Whitaker JW, Schultz MD, Ward LD, Sarkar A, Quon G, Sandstrom RS, Eaton ML, Wu YC, Pfenning AR, Wang X, Claussnitzer M, Liu

Y, Coarfa C, Harris RA, Shoresh N, Epstein CB, Gjoneska E, Leung D, Xie W, Hawkins RD, Lister R, Hong C, Gascard P, Mungall AJ, Moore R, Chuah E, Tam A, Canfield TK, Hansen RS, Kaul R, Sabo PJ, Bansal MS, Carles A, Dixon JR, Farh KH, Feizi S, Karlic R, Kim AR, Kulkarni A, Li D, Lowdon R, Elliott G, Mercer TR, Neph SJ, Onuchic V, Polak P, Rajagopal N, Ray P, Sallari RC, Siebenthall KT, Sinnott-Armstrong NA, Stevens M, Thurman RE, Wu J, Zhang B, Zhou X, Beaudet AE, Boyer LA, De Jager PL, Farnham PJ, Fisher SJ, Haussler D, Jones SJ, Li W, Marra MA, McManus MT, Sunyaev S, Thomson JA, Tlsty TD, Tsai LH, Wang W, Waterland RA, Zhang MQ, Chadwick LH, Bernstein BE, Costello JF, Ecker JR, Hirst M, Meissner A, Milosavljevic A, Ren B, Stamatoyannopoulos JA, Wang T, Kellis M; Roadmap Epigenomics Consortium. Integrative analysis of 111 reference human epigenomes. *Nature*. 2015;**518**(7539):317–330.

21. Barreto RS, Bressan FF, Oliveira LJ, Pereira FT, Perecin F, Ambrósio CE, Meirelles FV, Miglino MA. Gene expression in placentation of farm animals: an overview of gene function during development. *Theriogenology*. 2011;**76**(4):589–597.
22. Zhou Y, Gormley MJ, Hunkapiller NM, Kapidzic M, Stolyarov Y, Feng V, Nishida M, Drake PM, Bianco K, Wang F, McMaster MT, Fisher SJ. Reversal of gene dysregulation in cultured cytotrophoblasts reveals possible causes of preeclampsia. *J Clin Invest*. 2013;**123**(7):2862–2872.
23. Tilburgs T, Crespo AC, van der Zwan A, Rybalov B, Raj T, Stranger B, Gardner L, Moffett A, Strominger JL. Human HLA-G+ extravillous trophoblasts: immune-activating cells that interact with decidual leukocytes. *Proc Natl Acad Sci USA*. 2015;**112**(23):7219–7224.
24. Fisher SJ, Cui TY, Zhang L, Hartman L, Grahl K, Zhang GY, Tarpey J, Damsky CH. Adhesive and degradative properties of human placental cytotrophoblast cells in vitro. *J Cell Biol*. 1989;**109**(2):891–902.
25. McMaster MT, Librach CL, Zhou Y, Lim KH, Janatpour MJ, DeMars R, Kovats S, Damsky C, Fisher SJ. Human placental HLA-G expression is restricted to differentiated cytotrophoblasts. *J Immunol*. 1995;**154**(8):3771–3778.
26. Maldonado-Estrada J, Menu E, Roques P, Barré-Sinoussi F, Chaouat G. Evaluation of cytokeratin 7 as an accurate intracellular marker with which to assess the purity of human placental villous trophoblast cells by flow cytometry. *J Immunol Methods*. 2004;**286**(1-2):21–34.
27. Kovats S, Main EK, Librach C, Stubblebine M, Fisher SJ, DeMars R. A class I antigen, HLA-G, expressed in human trophoblasts. *Science*. 1990;**248**(4952):220–223.
28. Kaya B, Nayki U, Nayki C, Ulug P, Oner G, Gultekin E, Yildirim Y. Proliferation of trophoblasts and Ki67 expression in preeclampsia. *Arch Gynecol Obstet*. 2015;**291**(5):1041–1046.
29. Winn VD, Haimov-Kochman R, Paquet AC, Yang YJ, Madhusudhan MS, Gormley M, Feng KT, Bernlohr DA, McDonagh S, Pereira L, Sali A, Fisher SJ. Gene expression profiling of the human maternal-fetal interface reveals dramatic changes between midgestation and term. *Endocrinology*. 2007;**148**(3):1059–1079.
30. Saeed AI, Bhagabati NK, Braisted JC, Liang W, Sharov V, Howe EA, Li J, Thiagarajan M, White JA, Quackenbush J. TM4 microarray software suite. *Methods Enzymol*. 2006;**411**:134–193.
31. Huang DW, Sherman BT, Tan Q, Kir J, Liu D, Bryant D, Guo Y, Stephens R, Baseler MW, Lane HC, Lempicki RA. DAVID Bioinformatics Resources: expanded annotation database and novel algorithms to better extract biology from large gene lists. *Nucleic Acids Res*. 2007;**35**(Web Server issue):W169–W175.
32. Robinson JF, Verhoef A, van Beelen VA, Pennings JL, Piersma AH. Dose-response analysis of phthalate effects on gene expression in rat whole embryo culture. *Toxicol Appl Pharmacol*. 2012;**264**(1):32–41.
33. Team RC. *R: A Language and Environment for Statistical Computing*. Vienna: R Foundation for Statistical Computing; 2014.
34. Zhou Y, McMaster M, Woo K, Janatpour M, Perry J, Karpanen T, Alitalo K, Damsky C, Fisher SJ. Vascular endothelial growth factor ligands and receptors that regulate human cytotrophoblast survival are dysregulated in severe preeclampsia and hemolysis, elevated liver enzymes, and low platelets syndrome. *Am J Pathol*. 2002;**160**(4):1405–1423.
35. Hromatka BS, Drake PM, Kapidzic M, Stolp H, Goldfien GA, Shih IeM, Fisher SJ. Polysialic acid enhances the migration and invasion of human cytotrophoblasts. *Glycobiology*. 2013;**23**(5):593–602.
36. Luo J, Qiao F, Yin X. Impact of silencing MMP9 gene on the biological behaviors of trophoblasts. *J Huazhong Univ Sci Technolog Med Sci*. 2011;**31**(2):241–245.
37. Librach CL, Werb Z, Fitzgerald ML, Chiu K, Corwin NM, Esteves RA, Grobelny D, Galardy R, Damsky CH, Fisher SJ. 92-kD type IV collagenase mediates invasion of human cytotrophoblasts. *J Cell Biol*. 1991;**113**(2):437–449.
38. Plaks V, Rinkenberger J, Dai J, Flannery M, Sund M, Kanasaki K, Ni W, Kalluri R, Werb Z. Matrix metalloproteinase-9 deficiency phenocopies features of preeclampsia and intrauterine growth restriction. *Proc Natl Acad Sci USA*. 2013;**110**(27):11109–11114.
39. Kolben M, Lopens A, Bläser J, Ulm K, Schmitt M, Schneider KT, Tschesche H. Proteases and their inhibitors are indicative in gestational disease. *Eur J Obstet Gynecol Reprod Biol*. 1996;**68**(1-2):59–65.
40. Rahimi Z, Rahimi Z, Shahsavandi MO, Bidoki K, Rezaei M. MMP-9 (-1562 C:T) polymorphism as a biomarker of susceptibility to severe pre-eclampsia. *Biomarkers Med*. 2013;**7**(1):93–98.
41. Aplin JD, Jones CJ, Harris LK. Adhesion molecules in human trophoblast: a review. I. Villous trophoblast. *Placenta*. 2009;**30**(4):293–298.
42. Harris LK, Jones CJ, Aplin JD. Adhesion molecules in human trophoblast: a review. II. Extravillous trophoblast. *Placenta*. 2009;**30**(4):299–304.
43. Damsky CH, Librach C, Lim KH, Fitzgerald ML, McMaster MT, Janatpour M, Zhou Y, Logan SK, Fisher SJ. Integrin switching regulates normal trophoblast invasion. *Development*. 1994;**120**(12):3657–3666.
44. Takai N, Ueda T, Narahara H, Miyakawa I. Expression of c-Ets1 protein in normal human placenta. *Gynecol Obstet Invest*. 2006;**61**(1):15–20.
45. Kessler CA, Stanek JW, Stringer KF, Handwerger S. ETS1 induces human trophoblast differentiation. *Endocrinology*. 2015;**156**(5):1851–1859.
46. Cervar M, Puerstner P, Kainer F, Desoye G. Endothelin-1 stimulates the proliferation and invasion of first trimester trophoblastic cells in vitro: a possible role in the etiology of pre-eclampsia? *J Investig Med*. 1996;**44**(8):447–453.
47. Hiden U, Bilban M, Knöfler M, Desoye G. Kisspeptins and the placenta: regulation of trophoblast invasion. *Rev Endocr Metab Disord*. 2007;**8**(1):31–39.
48. Takahashi H, Takizawa T, Matsubara S, Ohkuchi A, Kuwata T, Usui R, Matsumoto H, Sato Y, Fujiwara H, Okamoto A, Suzuki M, Takizawa T. Extravillous trophoblast cell invasion is promoted by the CD44-hyaluronic acid interaction. *Placenta*. 2014;**35**(3):163–170.
49. Fan X, Rai A, Kambham N, Sung JF, Singh N, Petitt M, Dhal S, Agrawal R, Sutton RE, Druzin ML, Gambhir SS, Ambati BK, Cross JC, Nayak NR. Endometrial VEGF induces placental sFLT1 and leads to pregnancy complications. *J Clin Invest*. 2014;**124**(11):4941–4952.
50. Jovanović M, Vićovac L. Interleukin-6 stimulates cell migration, invasion and integrin expression in HTR-8/SVneo cell line. *Placenta*. 2009;**30**(4):320–328.
51. Zhang H, Hou L, Li CM, Zhang WY. The chemokine CXCL6 restricts human trophoblast cell migration and invasion by suppressing MMP-2 activity in the first trimester. *Hum Reprod*. 2013;**28**(9):2350–2362.
52. De-Regil LM, Palacios C, Lombardo LK, Peña-Rosas JP. Vitamin D supplementation for women during pregnancy. *Cochrane Database Syst Rev*. 2016;**1**(1):CD008873.
53. Wei SQ. Vitamin D and pregnancy outcomes. *Curr Opin Obstet Gynecol*. 2014;**26**(6):438–447.

54. Mislanova C, Martsenyuk O, Huppertz B, Obolenskaya M. Placental markers of folate-related metabolism in preeclampsia. *Reproduction*. 2011;**142**(3):467–476.
55. Chan SY, Susarla R, Canovas D, Vasilopoulou E, Ohizua O, McCabe CJ, Hewison M, Kilby MD. Vitamin D promotes human extravillous trophoblast invasion in vitro. *Placenta*. 2015;**36**(4): 403–409.
56. O'Brien KO, Li S, Cao C, Kent T, Young BV, Queenan RA, Pressman EK, Cooper EM. Placental CYP27B1 and CYP24A1 expression in human placental tissue and their association with maternal and neonatal calcitropic hormones. *J Clin Endocrinol Metab*. 2014;**99**(4):1348–1356.
57. Ma R, Gu Y, Zhao S, Sun J, Groome LJ, Wang Y. Expressions of vitamin D metabolic components VDBP, CYP2R1, CYP27B1, CYP24A1, and VDR in placentas from normal and preeclamptic pregnancies. *Am J Physiol Endocrinol Metab*. 2012;**303**(7): E928–E935.
58. Nuño-Ayala M, Guillén N, Arnal C, Lou-Bonafonte JM, de Martino A, García-de-Jalón JA, Gascón S, Osaba L, Osada J, Navarro MA. Cystathionine β-synthase deficiency causes infertility by impairing decidualization and gene expression networks in uterus implantation sites. *Physiol Genomics*. 2012;**44**(14): 702–716.
59. Nebert DW, Dalton TP. The role of cytochrome P450 enzymes in endogenous signalling pathways and environmental carcinogenesis. *Nat Rev Cancer*. 2006;**6**(12):947–960.
60. Liu H, Koukoulas I, Ross MC, Wang S, Wintour EM. Quantitative comparison of placental expression of three aquaporin genes. *Placenta*. 2004;**25**(6):475–478.
61. Prat C, Bouvier D, Comptour A, Marceau G, Belville C, Clairefond G, Blanc P, Gallot D, Blanchon L, Sapin V. All-trans-retinoic acid regulates aquaporin-3 expression and related cellular membrane permeability in the human amniotic environment. *Placenta*. 2015; **36**(8):881–887.
62. Guo J, Tian T, Lu D, Xia G, Wang H, Dong M. Alterations of maternal serum and placental follistatin-like 3 and myostatin in preeclampsia. *J Obstet Gynaecol Res*. 2012;**38**(7):988–996.
63. March MI, Geahchan C, Wenger J, Raghuraman N, Berg A, Haddow H, Mckeon BA, Narcisse R, David JL, Scott J, Thadhani R, Karumanchi SA, Rana S. Circulating angiogenic factors and the risk of adverse outcomes among Haitian women with preeclampsia. *PLoS One*. 2015;**10**(5):e0126815.
64. Aghababaei M, Beristain AG. The Elsevier Trophoblast Research Award Lecture: Importance of metzincin proteases in trophoblast biology and placental development: a focus on ADAM12. *Placenta*. 2015;**36**(Suppl 1):S11–S19.
65. Zhou Q, Xiong Y, Chen Y, Du Y, Zhang J, Mu J, Guo Q, Wang H, Ma D, Li X. Effects of tissue factor pathway inhibitor-2 expression on biological behavior of BeWo and JEG-3 cell lines. *Clin Appl Thromb Hemost*. 2012;**18**(5):526–533.
66. Xiong Y, Zhou Q, Jiang F, Zhou S, Lou Y, Guo Q, Liang W, Kong D, Ma D, Li X. Changes of plasma and placental tissue factor pathway inhibitor-2 in women with preeclampsia and normal pregnancy. *Thromb Res*. 2010;**125**(6):e317–e322.
67. Fong FM, Sahemey MK, Hamedi G, Eyitayo R, Yates D, Kuan V, Thangaratinam S, Walton RT. Maternal genotype and severe preeclampsia: a HuGE review. *Am J Epidemiol*. 2014;**180**(4):335–345.
68. Ishibashi O, Ohkuchi A, Ali MM, Kurashina R, Luo SS, Ishikawa T, Takizawa T, Hirashima C, Takahashi K, Migita M, Ishikawa G, Yoneyama K, Asakura H, Izumi A, Matsubara S, Takeshita T, Takizawa T. Hydroxysteroid (17-β) dehydrogenase 1 is dysregulated by miR-210 and miR-518c that are aberrantly expressed in preeclamptic placentas: a novel marker for predicting preeclampsia. *Hypertension*. 2012;**59**(2):265–273.
69. Chung TW, Park MJ, Kim HS, Choi HJ, Ha KT. Integrin αVβ3 and αVβ5 are required for leukemia inhibitory factor-mediated the adhesion of trophoblast cells to the endometrial cells. *Biochem Biophys Res Commun*. 2016;**469**(4):936–940.
70. Kakugawa S, Langton PF, Zebisch M, Howell SA, Chang TH, Liu Y, Feizi T, Bineva G, O'Reilly N, Snijders AP, Jones EY, Vincent JP. Notum deacylates Wnt proteins to suppress signalling activity. *Nature*. 2015;**519**(7542):187–192.
71. Zhang X, Cheong SM, Amado NG, Reis AH, MacDonald BT, Zebisch M, Jones EY, Abreu JG, He X. Notum is required for neural and head induction via Wnt deacylation, oxidation, and inactivation. *Dev Cell*. 2015;**32**(6):719–730.
72. Sonderegger S, Husslein H, Leisser C, Knofler M. Complex expression pattern of Wnt ligands and frizzled receptors in human placenta and its trophoblast subtypes. *Placenta* 2007;**28**(Suppl A):S97–S102.
73. Wang Z, Cao CJ, Huang LL, Ke ZF, Luo CJ, Lin ZW, Wang F, Zhang YQ, Wang LT. EFEMP1 promotes the migration and invasion of osteosarcoma via MMP-2 with induction by AEG-1 via NF-κB signaling pathway. *Oncotarget*. 2015;**6**(16):14191–14208.
74. Yang T, Zhang H, Qiu H, Li B, Wang J, Du G, Ren C, Wan X. EFEMP1 is repressed by estrogen and inhibits the epithelial-mesenchymal transition via Wnt/β-catenin signaling in endometrial carcinoma. *Oncotarget*. 2016;**7**(18):25712–25725.
75. Moore RM, Redline RW, Kumar D, Mercer BM, Mansour JM, Yohannes E, Novak JB, Chance MR, Moore JJ. Differential expression of fibulin family proteins in the para-cervical weak zone and other areas of human fetal membranes. *Placenta*. 2009;**30**(4): 335–341.